



Universität für Bodenkultur Wien

## Department of material sciences and process engineering (MAP)

Institute of wood technology and renewable materials

*Head of the institute:* Univ.Prof.Dipl.-Ing.Dr.nat.techn. Wolfgang Gindl-  
Altmutter

*Supervisor:* Univ.Prof.Dipl.-Ing.Dr.nat.techn.Dr.h.c Alfred Teischinger

*Co-supervisor:* Ing. Robert Stingl

## Drying properties of wet-glued large-sized construction spruce lumber

Master Thesis

for obtaining a Master's degree at the University of Natural Resources  
and Life Sciences, Vienna

*Submitted by*

Marko Kovačević

Vienna, 9 June 2017

## Abstract

This study is part of an extensive project of the international company *Stora Enso Wood Products*. The aim of the project is to develop a new wet-glued large-sized structural wood product that would both greatly improve raw material efficiency and decrease some negative effects of anisotropy and inconsistency of physical and mechanical properties of a traditional wood product. The thesis focuses on convective drying of large-sized cross-section construction lumber using conventional temperatures, with the focal point being the wet-glued product. The objective is primarily to determine whether drying of this new product is possible using traditional drying methods, and if so whether it is feasible to achieve target moisture content in comparable time to traditional, non-glued lumber. Much of time and attention was dedicated to observing and analyzing moisture gradients of non-glued and glued timber, in order to compare their drying manner and speed as well as identifying flaws in the traditional drying schedule. Twist and bow deformation were measured and examined, along with cross-sectional deformation and consequential material loss. At the end of each drying schedule a measurement of checks was taken and further analyzed for both non-glued and glued tested units.

Drying was conducted in two laboratory-scale, compartment, conventional temperature kilns with automatic drying regime control. Four runs were conducted in total. The first batch was dried in the larger kiln, *Mühlböck*, with the timber length of 1,5 m. The following three batches were dried in a smaller kiln, *Vanicek*, with a drying unit length of 0,5 m. 69 units were dried in total. Drying schedules were rather harsh compared to those from referenced literature. Two different methods were used for moisture content measuring - resistance and gravimetric. Afterwards, comparison and analysis of the two methods were performed.

The results showed quite a similar drying manner of non-glued and glued timbers. Very similar drying rates of both groups of timbers were recorded for units with similar basic density, initial moisture content and moisture distribution. However, these three parameters considerably influenced the drying rate in both groups. A slight obstacle for moisture diffusion due to narrowing of glue lines was observed. Nevertheless, this effect was negligible, since moisture content of wood at the narrowest part of the corresponding section, near the pith, was always low. Moreover, relatively mild parameter changes in drying schedules had no notable effect.

Great differences among gravimetric and resistance methods were observed, consequently questioning traditional measuring of moisture in kilns and control of drying schedule based on average moisture content when drying large-sized cross-section lumber. Unreliable on-line measuring using the resistance method was the chief reason for over-drying of almost all timbers. The use of mean moisture content to control drying schedules gives satisfying results when drying thin boards, since moisture gradients are lower. However, when drying thick timbers the problem has to be differently addressed.

Alternating position of the sections in glued units had a very positive effect on the shape stability of timbers. The negative effect of pith was almost completely neutralized. Both twist and bow deformation were lower compared to non-glued units. Moreover, considerably lesser cross-sectional deformation of glued units was recorded. The mean loss of dried material solely due to this deformation, not taking into account twist and bow, was 2,7 % lower for glued timbers.

Quite a high amount of checks on both non-glued and glued timbers was observed due to a rather severe drying schedule. In general, non-glued timbers were less prone to checking than glued ones. This was most likely due to almost pure tangential shrinkage in one of the two orthogonal directions of the cross-section of timber. The increase in checks, however, was not major. Furthermore, non-glued timbers had wider checks in general, reaching up to 10 mm for timbers containing pith, compared to maximal 2 mm for glued units. Position of checks was highly dependent on the previous position in the cross-section of the log, making glued timbers much more consistent and predictive. Moreover, negative effect of pith and knots was evidently reduced due to the alternating pattern of adjacent sections of glued timbers, exhibiting for the

greatest part clear checks due to tangential shrinkage. Both of the mentioned aspects should facilitate focusing on future drying schedule optimization.

## Acknowledgements

Many thanks and great appreciation to my supervisor, Professor Alfred Teischinger, and co-supervisor, Mr. Robert Stingl, for the guidance, frequent help and valuable support throughout my thesis. I would also like to thank all the people from the Institute of Wood Technology and Renewable Materials, BOKU University, who were involved in this project.

I would like to express my sincere gratitude to Mr. Markus Hirmke from Stora Enso for the many insightful conversations, comments and suggestions. My thanks to Mr. Peter Wagner for his contribution and to Stora Enso for funding this research.

Finally, my deep gratitude to my wife, parents, and my brother for unfailing support and encouragement throughout my studies.

## Table of content

1	Introduction .....	1
1.1	The aim of the study - objectives .....	1
2	Theoretical background to moisture movement during drying	
2.1	Liquid flow .....	2
2.2	Water diffusion .....	3
2.3	Vapor movement.....	5
2.4	Drying phases .....	5
2.5	Pit aspiration .....	6
3	Literature review .....	8
4	Materials and methods .....	12
4.1	Materials .....	12
4.1.1	Overall characterization of the material.....	12
4.1.2	Material density.....	13
4.2	Methods .....	13
4.2.1	The drying process.....	13
4.2.1.1	Schedule 1 .....	14
4.2.1.2	Schedules 2, 3 and 4.....	14
4.2.2	Moisture measurements and moisture profiles.....	15
4.2.2.1	Resistance method.....	15
4.2.2.2	Gravimetric method and moisture profiles.....	15
4.2.3	Conditioning.....	17
4.2.4	Twist and bow .....	17
4.2.5	Case-hardening .....	18
4.2.6	Cross-section scanning and material loss assessment .....	18
4.2.7	Checks.....	19
5	Results .....	20
5.1	Parameters for drying.....	20
5.2	Moisture content .....	21
5.2.1	Drying trends .....	21
5.2.1.1	The gravimetric method.....	21
5.2.1.2	Resistance vs gravimetric methods – comparison.....	25
5.2.2	Average moisture content at the end of drying.....	26
5.2.3	Moisture distribution and moisture gradients.....	26
5.2.4	Specimens 2 and 3 .....	32
5.3	Twist and bow .....	35
5.3.1	Twist .....	35
5.3.2	Bow .....	36
5.4	Material loss due to cross-sectional deformation .....	36
5.5	Case-hardening .....	38
5.6	Checks .....	38
5.6.1	Surface checks .....	38
5.6.2	End checks .....	40

5.6.3	Frequency of checks and length classification .....	41
5.6.4	Distribution of checks and general description .....	42
<b>6</b>	<b>Discussion .....</b>	<b>44</b>
6.1	Schedule .....	44
6.2	Drying.....	44
6.3	The effect of glue lines .....	45
6.4	Resistance vs gravimetric method .....	46
6.5	Checks and internal stresses .....	47
<b>7</b>	<b>Conclusion .....</b>	<b>49</b>
7.1	Further research .....	49
<b>8</b>	<b>References .....</b>	<b>51</b>

## Table of figures

Figure 2.1. A capillary tube, with a bubble of entrapped gas. ....	3
Figure 2.2. Hypothetical model for interpreting the effect of moisture distribution in the cell wall on the energy levels $H_a$ , $H_w$ , $H_s$ , and activation energy $E_s$ , for the case of: a – non-uniform moisture distribution, b – am uniform moisture distribution. (Skaar 1988).....	4
Figure 2.3. Calculated curves of the transverse bound water diffusion coefficient $D$ (log scale) as linear function of wood moisture content $M$ for several temperatures. (Skaar 1988).....	4
Figure 2.4 Conceptual model of a <i>Picea glauca</i> or <i>Picea mariana</i> tracheid bordered pit pair. (Schulte et al. 2015).....	6
Figure 2.5. Unaspirated bordered pit in a sapwood thacheid of <i>Tsuga canadensis</i> . (Siau 1984).....	7
Figure 2.6. Heavily aspirated bordered pit pair in the heartwood region of <i>Pinus rigida</i> . (Siau 1984).....	7
Figure 3.1. The evolution of stresses during drying of a 90 mm thick (D90) and 30 mm thick (D30) board. (Rémond 2004). ....	10
Figure 4.1. The cross-section of a non-glued timber. ....	12
Figure 4.2. The cross-section of a glued timber with distinct annual ring pattern. ....	12
Figure 4.3. The larger kiln, Mühlböck, and first drying batch.....	14
Figure 4.4. A follow-up timber for further analysis. ....	16
Figure 4.5. Specimen 1 – moisture gradient assessment. ....	16
Figure 4.6. Three-point measuring device for twist deformation assessment. ....	17
Figure 4.7. Bow deformation measuring ( $h$ – pitch at 1m length).....	18
Figure 4.8. A device for case-hardening evaluation (according to ÖNORM ENV 14464). ....	18
Figure 5.1. Temperature trend - Schedule 2. ....	20
Figure 5.2. Actual moisture content to equilibrium moisture content ( $T_g$ ) – Schedule 2. ....	21
Figure 5.3. Specimen 1 – A specimen used for moisture content and moisture distribution assessment. ....	22
Figure 5.4. Cross-section of a glued timber in “green” state. ....	22
Figure 5.5. Moisture content measurements during schedules 2 to 4 (resistance “–” and gravimetric “grav.” methods). ....	23
Figure 5.6. Drying trend for segments 1, 5 and 9; non-glued timber N4 - run 2; comparison of resistance (line) and gravimetric (dots) method. ....	24
Figure 5.7. Drying trend for segments 1, 5 and 9; glued timber 70B - run 2; comparison of resistance (line) and gravimetric (dots) method. ....	24
Figure 5.8. Drying according to resistance method - Timbers with high initial moisture content. (resistant – lines; gravimetric – dots).....	25
Figure 5.9. Moisture content at the end of kiln-drying - non-glued timbers (Schedules 1 - 4). ....	26
Figure 5.10. Moisture content at the end of kiln-drying - glued timbers (Schedules 1 - 4). ....	26
Figure 5.11. Moisture gradients evaluated at intervals from the beginning to the end of drying - glued timber 39B - run3. ....	27
Figure 5.12. Moisture gradients evaluated at intervals from the beginning to the end of drying - non-glued timber N3 - run 4G - "Specimen 1". ....	28
Figure 5.13. Moisture gradients evaluated at intervals from the beginning to the end of drying - glued timber 70B - run 4G - "Specimen 1". ....	28
Figure 5.14. Moisture gradients at the end of kiln-drying colored by batch*; Schedules 2, 3 and 4. ....	29
Figure 5.15. Moisture gradients at the end of kiln-drying colored by stem*; Schedules 2, 3 and 4. ....	29

Figure 5.16. Min, mean and max moisture contents - non-glued timbers - end of kiln drying (runs 2 to 4).	30
Figure 5.17. Min, mean and max moisture contents - glued timbers - end of kiln drying (runs 2 to 4).	30
Figure 5.18. Min, mean and max moisture contents - non-glued timbers - end of conditioning (runs 2 and 3).	31
Figure 5.19. Min, mean and max moisture contents - glued timbers - end of conditioning (runs 2 and 3).	31
Figure 5.20. Moisture gradients from the beginning to the end of drying - non-glued timber N3 - run 4G - "Specimen 1".	31
Figure 5.21. Moisture gradients from the beginning to the end of drying - glued timber 70B - run 4G - "Specimen 1".	31
Figure 5.22. Specimen 2	32
Figure 5.23. Specimen 3	32
Figure 5.24. Moisture content of segments I, II, III and IV at the end of kiln-drying - Specimen 3.	33
Figure 5.25. Drying curves - Segments I, II, III and IV - Specimen 3 (dots – gravimetric measurements; dotted lines – polynomial fit).	34
Figure 5.26. Twist evaluation during drying – non-glued timbers.	35
Figure 5.27. Twist evaluation during drying – glued timbers.	35
Figure 5.28. Twist at the end of Schedule 1 - non-glued timbers.	35
Figure 5.29. Twist at the end of Schedule 1 - glued timbers.	36
Figure 5.30. Bow - non-glued and glued timbers - Schedule 1.	36
Figure 5.31. Material loss due to deformation of the cross-section; Quartiles.	37
Figure 5.32. A scan of the cross-section for material loss assessment (non-glued).	37
Figure 5.33. A scan of the cross-section for material loss evaluation (glued).	37
Figure 5.34. Case-hardening after one day conditioning (batches 2, 3 and 4); Quartiles.	38
Figure 5.35. Case-hardening after 5 days conditioning (batch 4); Quartiles.	38
Figure 5.36. Length of Surface Checks per Timber - Quartiles (Schedules 1* to 4).	39
Figure 5.37. A typical diagonally-oriented inner check in a non-glued timber.	39
Figure 5.38. Lengths of surface checks per type and timber - Non-glued timbers (Schedules 1 to 4).	40
Figure 5.39. Lengths of surface checks per type and timber - Glued timbers (Schedules 1 to 4).	40
Figure 5.40. Length of End Checks per Timber - Quartiles (Schedules 1 to 4).	40
Figure 5.41. Mean and median of end checks (summed lengths) per timber and schedule.	41
Figure 5.42. Average number of surface checks per length category and timber (Schedules 1* to 4).	41
Figure 5.43. Average number of end-checks per length category and timber (Schedules 1* to 4).	41
Figure 5.44. The share of surface checks (lengthwise) per side - Glued timbers (Schedules 1 to 4).	42
Figure 5.45. A typical position of checks in glued timbers.	42
Figure 5.46. A typical wide check in a pith-containing non-glued timber.	43

## Table of tables

<i>Table 1. Drying schedules used for drying timbers and beams in (Glos &amp; Wagner 1988)</i> .....	8
<i>Table 2. Drying schedules for thick lumber (Rémond 2004)</i> .....	11
<i>Table 3. Simulated drying duration and moisture content difference between the core and the surface of a 90 mm thick board. (Rémond 2004)</i> .....	11
<i>Table 4. Drying schedule used for the first and second batch.</i> .....	14
<i>Table 5. Drying schedule used for the fourth batch.</i> .....	15
<i>Table 6. Drying duration. Schedules 1-4.</i> .....	20

# 1 Introduction

A sawmill is a facility where a specific roundwood of a tree, cut to length as sawlogs is machined into lumber. Sawmilling is a type of primary wood processing with the objective to produce a desired shape and dimension of lumber out of the slightly conical geometry of a sawlog. Besides the geometry and dimension of the lumber, the surface quality and accuracy, the yield of lumber from the logs is one of the most important indicator of an economical viable process. Sawing types, which also contribute to an economical way of machining, are classified according to the basic machine design, that is, sash gang saws or frame saws, circular saws and band saws. Modern sawmill techniques combine a head rig or head saw system for primary log break down and a resaw for resawing cants into boards. Various textbooks cover the sawmilling process such as Fronius (1982; 1989; 1991) and Brackwell & Walker (2006). The general sequence of sawmilling process steps in lumber manufacture are debarking, primary log break down, resawing (secondary break down), trimming and edging, green sorting, stacking for drying and lumber drying. All lumber, however, does not necessarily go through all the steps.

A fairly low sawn goods yield together with wood anisotropy represent some of the most important challenges of sawmill and wood industry in general. Nowadays logs are indeed fully processed, and every part of them is eventually used. However, the fact that the share of high value products reaches only up to 65% of the whole production volume, even in the most productive sawmills (Walker 2006), is highly unsatisfying and unpromising from both economic and environmental perspectives.

This thesis is part of an extensive project of the international sawmill company *Stora Enso Wood Products*, a subsidiary of the *Stora Enso Group*. The project is based on ideas developed by Mr. Markus Hirmke and his fellow colleagues within *Stora Enso*. The aim of the project is to develop a new wet-glued wood product for the construction industry, which would be a step forward in resolving some of the problems mentioned above. The developed sawing pattern allows for a significant increase in the share of sawn goods in a log. In order to achieve this, the machined lumber pieces have to be wet-glued to specific large-sized dimensions prior to the drying process.

## 1.1 The aim of the study - objectives

This thesis focuses on convective kiln-drying of such large-sized structural wood components at conventional temperatures in the range of 65°C to 71°C. The focal point is on drying a wet glued product under development by *Stora Enso*, and specifically on its behavior during drying as compared to non-glued lumber of similar dimensions.

In the past lumber of large cross-sectional dimensions (130 cm x 130 cm and more) was stacked in green state and then left to air-drying. However, many large-scale sawmills have turned to technical kiln-drying. Some of the motives for such a trend are:

- considerably shorter intervals between production and end use, hence insufficient drying time after installing
- check and split formation after installing;
- rising customer demands and harder regulatory requirements regarding quality of products and lumber homogeneity
- fungal activity above 18 % moisture content;
- increased application of large sized wood products in surroundings of lower equilibrium moisture content due to architecture and environmental trends
- better moisture insulation of modern buildings, etc.

The thesis should answer the following questions:

- Is kiln-drying of the specific wet glued product possible with a conventional kiln-drying schedule?
- Can a target moisture content be reached within a comparable drying time to that of non-glued lumber of similar dimensions?
- Are moisture gradients higher?
- Is twist deformation mitigated?
- Is bow deformation reduced?
- Is waste of material due to cross-section deformation lowered?
- Is case-hardening lower?
- Are amount and extent of surface and end checks reduced?

In order to give an answer to these questions, glued and non-glued pieces (Figure 4.1, Figure 4.2) were dried together in four stacks, in two different laboratory-scaled kilns. Drying and evaluation were conducted at the *Institute of Wood Technology and Renewable Materials, BOKU University Vienna, in Tulln*.

## 2 Theoretical background to moisture movement during drying

Water in wood is present in three different forms: as free liquid in cell lumen, as hygroscopically bound water in cell walls and as vapor in cell lumens. While water in its liquid state is only present above the fiber saturation point (FSP), water vapor and bound water are present in all moisture contents. However, the only case when there is no water vapor is if lumens are completely filled with liquid (Hawley 1931). Depending on the forms mentioned above and moisture content there are several driving mechanisms affecting the moisture movement in wood.

“All three movements can take place simultaneously, however, in different parts of the same small piece of wood.”(Hawley 1931)

Wood drying process and wood-moisture relation are covered in various textbooks such as Teischinger (2012), Skaar (1988), Kolin (2000), Walker (2006), Simpson (1991) and Siau (1984).

### 2.1 Liquid flow

The most significant water driving force above FSP during drying is capillary tension on the surface between liquid and gas phase, whose intensity depends on the radius of the capillary. The liquid flow rate is, besides these forces, determined by permeability, which is the ability of wood to conduct fluids under a total pressure gradient (Skaar 1988). This mechanism is responsible for drying of the middle zone of a wood piece, despite being saturated (Kolin 2000; Hawley 1931). The capillary moisture movement is rather thoroughly described in (Hawley 1931) *Figure 2.1* shows a tube filled with water with an air bubble in it. This system is in equilibrium when the radius at  $a$  and  $c$  are the same and the radius of bubble  $b$ , if at atmospheric pressure, is the same. During drying water evaporates at the position  $a$ , moving the meniscus  $m$  toward the position  $a_1$ . Since the capillary tension is inversely correlated with the capillary radius, the tension at meniscus  $m$  increases, simultaneously forcing the meniscus  $n$  to move from point  $c$  toward  $c_1$  in order to reach the equilibrium state. If the radius at  $a_1$  is smaller than at  $c_1$ , the meniscus  $n$  will retreat toward  $m$ , and at the same time meniscus  $m$  will move back and forth, always keeping the radii of  $m$  and  $n$  the same (in equilibrium). On the other hand, if the radius at  $c_1$  is smaller than at  $a_1$ , only the meniscus  $m$  will, with evaporation, continuously move toward  $c_1$ . The same principle of capillary tension applies to a bubble of air in a liquid. If the capillary tension at  $a_1$  is high enough, it can expand the bubble  $b$ . In fact, since the dimensions of bordered pits in wood are so small, the tension is usually sufficient to expand

the bubble throughout the whole lumen, simultaneously pushing all the liquid phase out of it. As this happens, the menisci *m* and *n* are stationary. (Hawley 1931)

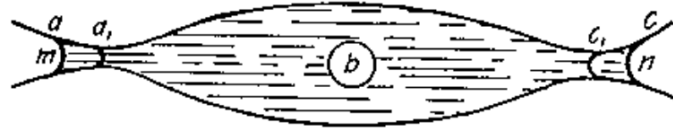


**Figure 2.1. A capillary tube, with a bubble of entrapped gas.**  
*a* - one aperture; *a1* - position of minimum radius of aperture *a*; *b* - bubble of entrapped air; *c* - the other aperture; *c1* - position of minimum radius of aperture *c*; *m* - meniscus at aperture *a*; *n* - meniscus at aperture *c*. (Hawley 1931)

## 2.2 Water diffusion

Bound-water movement through the cell wall is considered to be the major mechanism of moisture movement within the hygroscopic range. (Skaar 1988)

To quantify moisture diffusion in wood Fick's first law is usually used, which represents the relationship between the flux and the concentration gradient under steady-state conditions:

$$J = -D \left( \frac{\partial c}{\partial x} \right), \quad (1)$$

where *J* is the steady state flux of moisture, g/cm<sup>2</sup>,  $\partial c/\partial x$  is the concentration gradient of water in the wood and *D*, cm<sup>2</sup>/s, is the water diffusion coefficient of wood.

Siau (1984), Skaar (1988) and Vanek & Teischinger (1989) suggest that there are several alternative ways for quantifying moisture diffusion in the cell wall: vapor pressure, chemical potential and spreading pressure among others, each of them using a particular transport coefficient analogical to Fick's law diffusion coefficient *D* from Equation 1. More detailed information on each of these moisture diffusion models is presented in Skaar (1988).

Since the Fick's law does not always give satisfying estimate for different diffusion problems, alternative models were proposed. Gas diffusion, sorption diffusion and surface diffusion are considered. Moreover, binding forces of sorption, and temperature along the diffusion paths, in case of non-isothermal diffusion, are taken into account. However, in isothermal environment and at lower moisture gradients Fick's law gives quite a good approximation of moisture diffusion. (Vanek & Teischinger 1989)

Water molecules are attracted to sorption sites in the cell wall, which are mostly attributed to the polar hydroxyl groups. A single sorption site can attract up to several water molecules in its vicinity, depending on the moisture content of the wood. However, the exact maximal number of water molecules per sorption site and the number of sorption sites is unknown. Molecules continuously vibrate about the equilibrium position, and if their kinetic energy is sufficient they may jump to the neighboring sorption site or yet evaporate from the wood if the energy is even higher. The energy barrier required to be overcome in order to jump from one sorption site to another is called activation energy, *E<sub>s</sub>*, and it is moisture dependent. The barrier at sorption sites with higher moisture content is lower, meaning that the bonds between water molecules and wood are weaker than at sites with lower moisture content (MC) (Figure 2.2a). This determines the direction of moisture movement from sites with higher MC toward those with lower MC. However, it does not imply that there is no movement in the opposite direction. Some molecules in fact jump to sites with higher MC. Given that the energy barrier here is higher, the total number of molecules diffusing toward higher MC sites is lower. Therefore, the

higher the MC gradient would become, the higher the diffusion rates would be. Skaar points out that molecules move from one site to another even if there is no moisture gradient. However, since the amount of water moving in both directions is almost equal due to the same  $E_s$  (Figure 2.2b), it could be assumed that moisture content on the macroscopic level remains constant. (Skaar 1988)

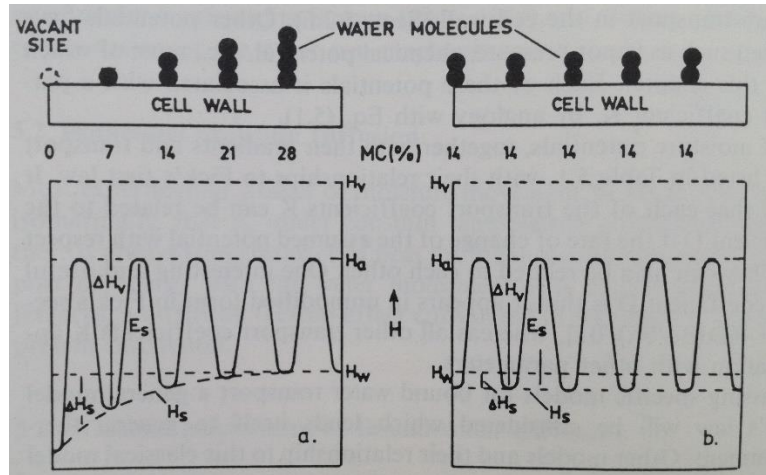


**Figure 2.2. Hypothetical model for interpreting the effect of moisture distribution in the cell wall on the energy levels  $H_a$ ,  $H_w$ ,  $H_s$ , and activation energy  $E_s$ , for the case of: a – non-uniform moisture distribution, b – a uniform moisture distribution. (Skaar 1988)**

With the influence of  $E_s$  already mentioned, it should be noted here that a slight change in moisture content, hence in activation energy  $E_s$  as well, causes a significant change in the diffusion coefficient  $D$  (Skaar 1988). This relationship is presented by Arrhenius equation:

$$D = D_0 \cdot \exp\left(\frac{-E_s}{R \cdot T}\right) \quad (2)$$

where  $D_0$  is a constant, dependent on the concentration and distribution of sorption sites,  $E_s$  is activation energy,  $R$  is the ideal gas constant, and  $T$  is temperature.

It is clear from the Arrhenius equation that, apart from the moisture content, temperature also has a strong impact on the diffusion coefficient (Figure 2.3). (Choong E T 1965; Siau 1984; Skaar 1988; Kang & Hart 1997).

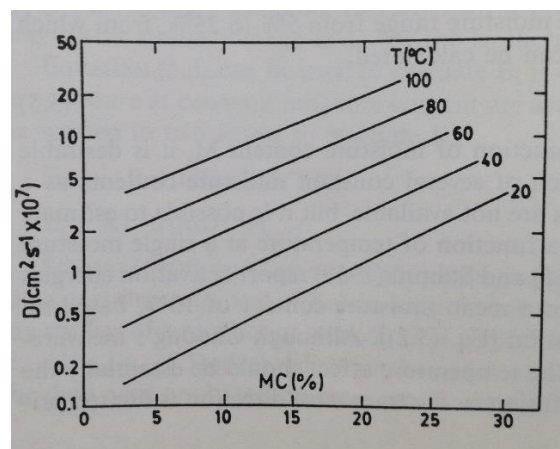


**Figure 2.3. Calculated curves of the transverse bound water diffusion coefficient  $D$  (log scale) as linear function of wood moisture content  $M$  for several temperatures. (Skaar 1988)**

## 2.3 Vapor movement

Other than liquid flow and bound water diffusion, vapor movement through cell cavities can play a significant role in total moisture transport, due to vapor pressure and total pressure gradients; its influence is especially evident at high drying temperatures and in woods with high permeability. (Choong E T 1965; Skaar 1988).

During high-temperature drying the vapor pressure could exceed the atmospheric pressure and as a consequence convective flow of vapor is dominant (Pang 1998). However, in the case of low-temperature drying, which is more common, the share of convective vapor flow is lower since the concentration of vapor in wood is much lower. In such situations both vapor diffusion and convective flow of air/vapor mixture affect vapor movement, with former becoming increasingly dominant with decreasing temperature. Pang (1998) calculated ratios of vapor diffusion to convective vapor flow at different drying temperatures. These are for example at 47 °C around 4,0, at 70 °C around 1,5 and at 100 °C circa 0,08. He pointed out, however, that these values should be considered as an approximation since several assumptions were made. It gives, though, a clear illustration of which mechanism plays a dominant role in vapor movement at different temperatures.

Pang (1998) proposed two drying models to predict drying of wood. The first one is simpler as it neglects vapor diffusion, and therefore would be more suitable for high temperature drying. The second is more complex, as it includes both vapor diffusion and convective flow, thus being able to offer good predictions for both high and low-temperature drying.

Contribution of vapor movement at lower temperatures and in transverse direction is much lower, since the vapor has cross walls on its way through the wood, with diffusion rates that are two or three orders of magnitude slower than the movement through the cell cavity (Choong E T 1965; Skaar 1988). Nevertheless, significance of wood species and variation in morphology should not be neglected. The experimental results of Mouchot et al. (2006) showed insignificant share of vapor diffusion in total diffusion for spruce wood in transverse directions, but accounted for 30 % of total diffusion in tangential and 10-15 % of total diffusion in radial direction for beech wood.

## 2.4 Drying phases

Depending on the dominant driving mechanism affecting moisture migration, three major drying periods may be distinguished when applying kiln-drying at conventional temperatures. The first phase, a pseudo-constant drying period (Rémond et al. 2005), is dominated by the capillary flow. Free water from inner zones of the drying unit supplies the evaporating front located near the wood surface. The term pseudo-constant comes from the fact that the evaporating front is not directly on the surface, but rather a “thin dry layer” is formed, which then expands at a very low rate (Rémond et al. 2005). Therefore, a slight yet negligible decrease in the drying rate is present. Formation of a thin dry layer is probably due to damaged surface layer and capillary network of the wood, caused by sawing (Salin 2010).

At some point the evaporation front starts to recede rapidly toward the central zones of the drying unit, due to insufficient capillary water supply. In this transitional phase, all of the three water migration mechanisms described above take place. Consequently, drying rate decreases as the share of moisture diffusion in the total moisture transport increases. Insufficient water supply is attributed to two factors: irreducible saturation, a state where liquid flow continuity is broken (Nijdam et al. 2000) and saturated tracheids are “trapped” by surrounding empty tracheids, and secondly to pit aspiration, which is discussed later. According to Wiberg & Moren (1999) this particular phase starts out in spruce wood at moisture content of around 60 %.

The third drying period is characterized by total absence of capillary flow, a dominating role of water diffusion, and the lowest drying rates of all three drying phases. It takes place when all parts of a drying unit are in the range under the fiber saturation point.

## 2.5 Pit aspiration

Softwood elements are interconnected by three types of pit pairs: simple, half-bordered, and bordered pit pair. The latter is responsible for connecting the fluid-conducting tissue, longitudinal and ray tracheids, which account to more than 95 % of softwood volume. Therefore, bordered pit pairs are considered as the most important for moisture flow of all three types of pit pairs. They consist of generally impermeable torus in the middle of the pit chamber, margo, and overarching borders (*Figure 2.4*). Margo, the tissue spreading from the torus to the periphery of the chamber, is composed of strand-like cellulose microfibrils allowing fluid flow between these strands (*Figure 2.4*). (Siau 1984)

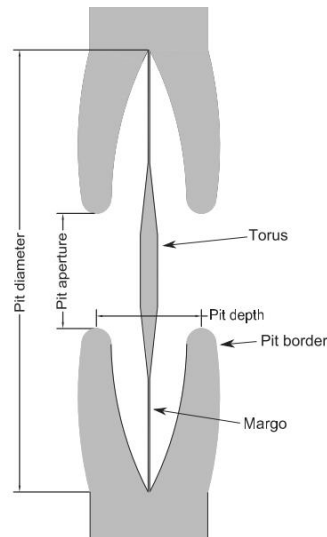


**Figure 2.4 Conceptual model of a *Picea glauca* or *Picea mariana* tracheid bordered pit pair. (Schulte et al. 2015)**

During drying, the torus is usually dislocated by surface tension of the evaporating liquid and held against the pit border, preventing liquid flow (*Figure 2.6*) (Siau 1984; Comstock & Côté 1968). This is called pit aspiration, and is considered to be the major factor in the reduction of softwood permeability (Usta & Hale 2006). According to Comstock & Côté (1968) there are three factors triggering the pit aspiration: surface tension, which forces torus toward the pit membrane; too low stiffness and rigidity of the membrane; adhesion between the torus and the border.

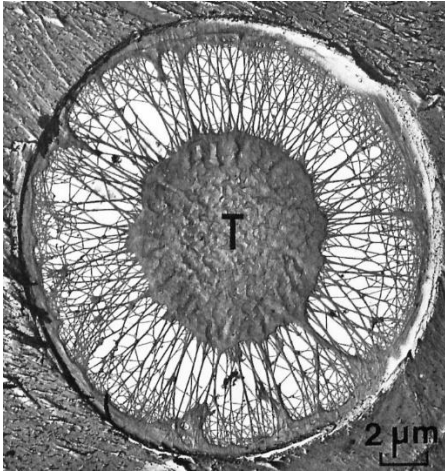


**Figure 2.5. Unspirated bordered pit in a sapwood thacheid of *Tsuga canadensis*. (Siau 1984)**

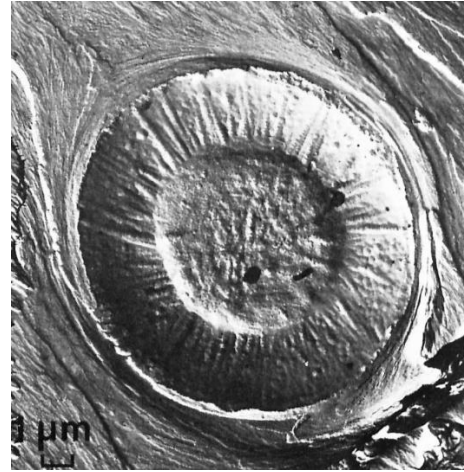


**Figure 2.6. Heavily aspirated bordered pit pair in the heartwood region of *Pinus rigida*. (Siau 1984)**

Pit aspiration is typical for some of commercially most valuable gymnosperms, *Pinaceae* family. The number of aspirated pits rises during drying with the decrease of moisture content to about fiber saturation point (Comstock & Côté 1968). However, permeability is in general slightly increased by further drying under the saturation point, due to shrinkage of the microfibrillar strands in the margo (Hansmann et al. 2002). While the earlywood pits are easily aspirated, latewood pits seem to be more resistant due to the thicker torus, tighter margo and smaller diameter (Rosner et al. 2010; Liese & Bauch 1967).

Liese & Bauch (1967) found that all earlywood and 80 to 85 % of pits in latewood tracheids of Norway spruce (*Picea abies*) were aspirated after drying. On the other hand, in the latewood of Scots pine (*Pinus sylvestris*) around 50 % of the membranes remained unspirated. The experiments of Comstock & Côté (1968) showed that temperature had a negative influence on pit aspiration. Permeability of Eastern hemlock (*Tsuga canadensis*) was lowered to only 1,5 % of its green wood value by drying at 70 °C. Surprisingly, even at -18 °C the permeability amounted to only 5 % of its original value. However, Usta & Hale (2006) obtained less dramatic results. After drying of Sitka (*Picea sitchensis*) and Eastern spruce (*Picea orientalis*), the share of aspirated pits amounted to 51 and 59 % respectively.

### 3 Literature review

Although there is plenty of literature regarding wood drying, the number of studies specifically addressing the problem of drying large dimensioned lumber is limited. Moreover, the majority of the literature available is written in German or French, and therefore out of the radar for many researches.

On the other hand, the topic of drying wet-glued large-sized construction lumber covered in this study has not been addressed yet.

A very extensive study on drying beams with a large cross section at conventional temperatures was conducted by Glos & Wagner (1988). In total 190 specimens of spruce wood were dried in six series. Cross-section dimensions of specimens were 8 cm x 16 cm and 14 cm x 26 cm. The length amounted 4 m in the first three stacks, and 2 m x 2 m in the last three. Influences of wood anatomy, cutting pattern, “relieving” grooves, as well as drying schedule on wood quality of dried specimens were investigated.

Two drying programs were used (*Table 1*). The first, labeled as normal, was applied to five batches. The second, classified as mild, was a two-cycle alternating program, implemented on the last series having only 14 cm x 26 cm specimens. The intervals of each cycle (drying and pause) were 1 hour until the moisture content of 30 % was reached, and 4 hours afterwards until the end of the program. Temperature was set to 65 °C at the beginning and 75°C at the end of each schedule. Drying time ranged between 329 and 446 hours.

**Table 1. Drying schedules used for drying timbers and beams in (Glos & Wagner 1988).**

Moisture content (%)	Glos (1988) - <i>normal</i>		Glos (1988) - <i>mild</i>	
	Dry-bulb temperature	EMC	EMC (cycle 1)	EMC2 (cycle 2)
< 60	65	12		
< 40	75	10.1	10,4	13,7
< 30	75	8.7	9	11.4
< 25	75	8.2	8.8	11.2
< 20	75	6.2	7.2	9.9
< 15	End	End	End	End

The influence of the pith on twist was considerable. Measurements of twist deformation on specimens containing pith were double as high as on specimens without pith. Furthermore, the dimensions of the cross-section affected the twist deformation significantly. Bigger specimens exhibited nearly 50 % lower twist than smaller ones. On the other hand, check formation was greater on bigger units.

The “relieving” grooves were introduced in an effort to mitigate drying stresses and consequently to improve wood quality. The grooves were centrally cut along the piece on both wider sides. They were 3 mm wide, and the depth was 20 % of the piece thickness (1,6 cm; 2,8 cm). No distinguishing impact on twist and bow was observed. However, a remarkable improvement in check formation was achieved. Not taking into account checks whose width was less than 1 mm, an impressive 80% of 14 cm x 26 cm specimens was check free, compared to only 20% for non-grooved units. It should be mentioned, though, that “residual thickness” of grooved specimens, the check-free thickness, was reduced compared to non-grooved units. The authors proposed a further investigation into the shape and dimensions of grooves to clarify this issue.

The mild drying program, with two alternating cycles, did not make any distinctive reductions in twist, bow or check formation. However, despite the pause of 170 hours, the schedule duration was comparable to that of *normal* schedules, opening the possibility for energy cost reduction.

Moisture gradients during drying, which would be additionally helpful for further schedule improvements, were not investigated or presented.

Welling & Mieth (1989) investigated the effect of round and slotted perforations on quality of dried lumber. The aim was to determine whether perforations in green lumber reduce depth of checks during drying. Moreover, the study investigated the influence of perforations on duration of drying. For round perforations needles with a diameter of 0,6 mm were inserted 1,0 cm into the wood with a concentration of 13.888 needles per m<sup>2</sup>. In total 140 two-meter-long specimens of three different cross-sections were dried together in three series. Dimensions of cross sections were as follows: 4 cm x 26 cm, 8 cm x 18 cm, 14 cm x 26 cm. Needles were used to make round perforations in lumber of the first two cross-section dimension, while slotted perforations were performed on specimens of third and the largest cross-section. For each batch a different drying program was conducted (A. air-drying; B. kiln-drying at a conventional temperature and C. alternate cycle kiln-drying). *Program B* was similar to that of (Glos & Wagner 1988). Parameters of *Program C* were set to match daily fluctuations in temperature and humidity during summer.

The reduction of check length was observed on every perforated specimen in each drying program. Nevertheless, the number of checks was much higher. According to Welling and Mieth, perforating weakens the wood in the surface zone, hence checks emerge at weak points before high stresses are developed. The total check length displayed no major improvements. No distinctive visual or aesthetic improvement was detected either. Only a slight reduction in depth and width of checks was achieved. Moreover, there was no record of a significant reduction in drying time. It was concluded, therefore, that additional production costs caused by perforation could not be justified.

Apart from the gravimetric method, moisture content (MC) measuring was done on-line using the resistance method on specimens of all three cross-sections. However, only one drying curve was displayed for all three cross-sections. Therefore, no conclusion could be drawn regarding drying rates of individual specimens. Furthermore, it was unclear whether the drying schedule was controlled by an average MC obtained from specimens of all three cross-sections or rather from the thickest cross-section.

Rémond (2004) used Patrick Perré's two-dimensional drying simulation code *Transpore* to address the problem of drying thick lumber. He initially used the code to track the state of drying stresses during drying and compare stress development in thick and thin spruce boards. Then, *Transpore* was used as a decision support to choose the more suitable schedule for drying a thick lumber among two schedules found in literature. Eventually, the code was used as a tool for improving the chosen schedule.

Drying of two boards, 90 mm and 30 mm thick, was simulated. In the first 12 hours of drying, the evaporative front (*Chapter 2.4*) of both boards moves equally slowly to around 3 mm beneath the wood surface, causing high tension in this narrow zone (*Figure 3.1*). Simultaneously, the saturated zone of the board is exposed to compression, to maintain the mechanical balance. During this interval there is no influence of board thickness; as a result both boards experience the same peak in tension. The compression in the thicker board is lower, though, since it is spread over the wider section within the piece. Furthermore, the central part of the thicker board remains under compression much longer (8 times longer, in this case). Afterwards, moisture from deeper zone of the thinner board becomes insufficient to supply the evaporation front with capillary water, its moisture gradient decreases and evaporative front moves quickly toward the core of the board. The consequential shrinking of deeper layers relieves the tension in the outer zone. Simultaneously, the stresses in the outer

zone of the thicker board continue to grow reaching a maximum that is greater than in the thinner board. Furthermore, the peripheral area under tension is much wider in the thicker than in the thinner board. This is of essential importance, since in the experimental part of the study the checks appeared only when a sufficiently wide zone was under tension. It should be mentioned, however, that after the reversal of stresses the core of the thinner board experiences slightly higher tension than the core of the thicker unit.

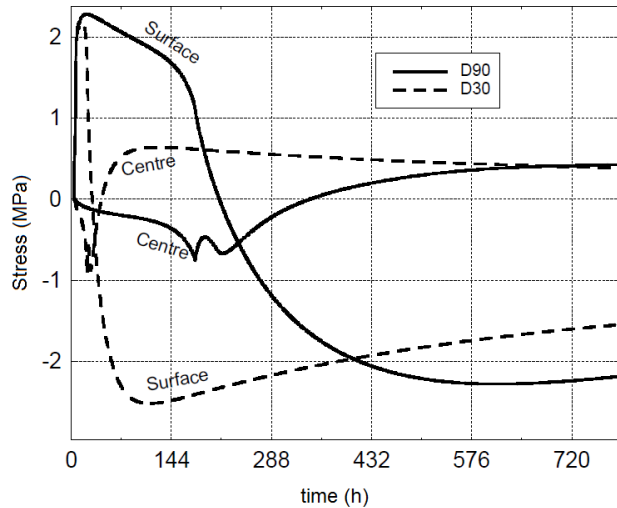


**Figure 3.1. The evolution of stresses during drying of a 90 mm thick (D90) and 30 mm thick (D30) board. (Rémond 2004).**

After simulating two drying schedules for thick lumber (*Table 2*), the form *Aleon* was chosen as more suitable for drying the thick lumber. Afterwards, *Transpore* was used for optimization of the chosen schedule (*Table 2*). The maximum tension in the outer zone of the board was lowered by approximately 20%, residual stresses were mitigated, as well as moisture gradients. On the other hand, the total duration of the schedule was slightly increased (*Table 3*). The table indicates that lessening harshness of the program does not necessarily mean prolonging the drying schedule.

**Table 2. Drying schedules for thick lumber (Rémond 2004).**

Moisture content (%)	Joly & More-Chevalier (1980)		Aléon et al. (1990)		Aléon et al. (1990) modified	
	Dry-bulb temperature	EMC	Dry-bulb temperature	EMC	Dry-bulb temperature	EMC
< 50	60	11				
< 40	60	10				
< 35			70	13.7	70	13.7
< 32			70	10.8	<del>70</del> 75	<del>10.8</del> 11.4
< 30	70	9	75	8.7	<del>75</del> 78	<del>8.7</del> 9.7
< 28			75	7.8	<del>75</del> 80	<del>7.8</del> 9
< 27	70	8				
< 25			75	6.5	<del>75</del> 80	<del>6.5</del> 8
< 24	70	7				
< 23						
< 21	70	6				
< 20			80	5	80	<del>5</del> 6.5
< 18	75	5				
< 15	75	4	80	3.8	80	3.8

**Table 3. Simulated drying duration and moisture content difference between the core and the surface of a 90 mm thick board. (Rémond 2004).**

		Joly & More-Chevalier (1980)	Aléon et al. (1990)	Aleon et al. (1990) modified
Flat sawn - heartwood	Time (h)	224	193	202
	Core MC – surface MC (%)	13.6	13	10.4
Quarter sawn – heartwood	Time (h)	195	169	178
	Core MC – surface MC (%)	13.3	13.1	10.2
Flat sawn - Sapwood	Time (h)	201	186	202
	Core MC – surface MC (%)	13	14	10.5

## 4 Materials and methods

### 4.1 Materials

#### 4.1.1 Overall characterization of the material

The product used in this study was developed by *Stora Enso* as a step forward in resolving problems such as very low raw material efficiency, as well as handling some of the negative effects of wood anisotropy. The product was made of Norway spruce wood (*Picea abies*), sawn using an unconventional and innovative cutting pattern (*Figure 4.2*) while gluing the pieces in a wet (green) condition using a one-component polyurethane adhesive. Just the wood surfaces intended for gluing were dried to moisture content just below 30 % prior to “wet-gluing” process. Delamination was not treated as a topic to be investigated in the current study. The position of annual rings of glued drying unit was always the same, having a radial cut on side surfaces and a tangential cut on upper and lower surface. Due to the specific cutting pattern, glued specimens did not include the pith and exhibit a typical growth-ring pattern.

Material was provided by *Stora Enso*, then brought to *The Institute of Wood Technology and Renewable Materials*, where it was cut to appropriate lengths; subsequent drying and measurements were conducted. Gluing was performed by *Stora Enso*.



**Figure 4.1.** The cross-section of a non-glued timber.

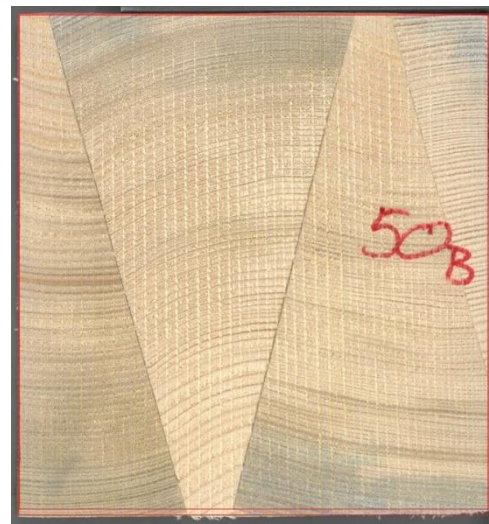


**Figure 4.2.** The cross-section of a glued timber with distinct annual ring pattern.

Apart from glued units, non-glued lumber was also used in the study in order to draw a precise comparison (*Figure 4.1*). They were made of Norway spruce wood from different parts of the stem, having an annual ring orientation as in *Figure 4.1*, with few of them even containing the pith.

The term *timbers* was used in this study to label both glued and non-glued drying units, since their cross-sectional dimensions complied with the *American Softwood Lumber Standard PS-20* (Ross 2010).

On the one hand, cross-sectional dimensions of glued timbers varied from 13 cm x 14,5 cm to 15 cm x 15 cm. On the other hand, all non-glued timbers had a cross-section of 15 cm x 15 cm. The length of each drying unit was 1,5 m in the first run and 0,5 m in the subsequent three batches (*Chapter 4.2.1.1*; *Chapter 4.2.1.2*) due to the availability of different laboratory dry-kilns at the institute.

Both non-glued and glued timbers were dried together in the same chamber, placed in an alternating sequence (glued – non-glued – glued etc.) with the aim of achieving a comparison as realistic as possible.

To reduce longitudinal over-drying, front sides were sealed either with aluminum foil or with resin, depending on whether the cross-cut was done at the institute (aluminum foil) or at Stora Enso (resin).

#### 4.1.2 Material density

The assessment of the basic density<sup>1</sup> was carried out on the specimens extracted from every single timber from the batches 2, 3 and 4 (except from the follow-up timbers - discussed later). The specimens, having corresponding cross-sections to the drying units and a thickness of 2 cm in grain direction (*Figure 5.32; Figure 5.33*), were extracted right after the drying schedule, but also once during (Schedules 2 and 3) and once after the conditioning phase (Schedules 2, 3 and 4) in order to obtain an average density which better corresponds to the density of the whole drying piece. In total 96 specimens were evaluated to obtain an estimated basic density of 36 drying units. It should be noted that the basic density is defined as the oven-dry mass of wood per unit volume in green state (Walker 2006), and hence gives lower values than oven-dry density. The measuring of the oven-dry mass of wood was conducted according to ÖNORM EN 13183-1.

Variation in density was considerable. Basic density of the sample ranged from 0,268 g/cm<sup>3</sup> to 0,385 g/cm<sup>3</sup> for non-glued timbers and from 0,314 g/cm<sup>3</sup> to 0,429 g/cm<sup>3</sup> for glued timbers; average density for the former was 0,326 g/cm<sup>3</sup> while it was 0,369 g/cm<sup>3</sup> for the latter.

## 4.2 Methods

### 4.2.1 The drying process

Drying was done in two laboratory-scale, compartment, conventional-temperature kilns of different capacities. Both kilns were equipped with a fully automatic control system provided by *Mühlböck*, where all necessary changes in the drying program were done automatically according to a pre-set schedule. Drying schedules were provided by *Stora Enso*.

Four runs were conducted in total. The first batch was dried in the larger kiln, *Mühlböck*, with the capacity of 1,5 m<sup>3</sup> and timber length of 1,5 m. The following three batches were dried in a smaller kiln, *Vanicek*. The capacity of this kiln was 0,15 m<sup>3</sup> with a drying unit length of 0,5 m. In total 69 timber pieces were dried.

All four runs were conducted at dry-bulb temperatures that were consistently kept at around 70 °C, with target moisture content of 15 %.

---

<sup>1</sup> The basic density was calculated retrospectively from the available data collected during the experiments.



**Figure 4.3.** The larger kiln, Mühlböck, and first drying batch.

#### 4.2.1.1 Schedule 1

The first run (*Schedule 1*) was carried out in the larger, *Mühlböck*, kiln (*Figure 4.3*). The pre-set drying schedule could be seen in *Table 4*. As the calculated average moisture content (MC) reached a specific value (*Chapter 4.2.2.1*), parameters (target dry-bulb temperature, wet-bulb temperature and air velocity) would change automatically. The program was rather harsh. Temperature increased gradually from 65 °C to 71 °C. *Trocknungsgefälle* (TG), a term often used in the German-speaking region, represented a ratio of MC of wood (with a maximum value of 30 %) to equilibrium MC, thus indicating the extent of severity of the drying program. TG was set to increase gradually from 3,3 at the beginning to 4,3 between MC of 46 % and 27 %, and then to steadily decrease to 2,9 at 15 %.

**Table 4.** Drying schedule used for the first and second batch.

Moisture content (%)	Dry-bulb temperature (°C)	Equilibrium MC (%)	TG (Trocknungsgefälle)
65	65	9	3,3
48	67	8	3,8
36	69	7,1	4,2
27	71	6,4	4,2
20	71	5,6	3,6
15	71	5,2	2,9

Initial dry-bulb temperature increase rate was set to 3 min/°C, after which the warm up stage was scheduled to last 7 hours at 10 % equilibrium MC.

#### 4.2.1.2 Schedules 2, 3 and 4

Since the second run (*Schedule 2*) was carried out in the smaller kiln, the same drying schedule was used as for the first batch (*Table 4*) in order to compare results from both kilns.

In contrast to the second batch, the third batch (*Schedule 3*) was exposed to an intermediate conditioning phase with the aim of lowering moisture gradients within timber. This phase was activated at an average MC of 25 %, its duration was 7 hours and TG was set to 2. The rest of the schedule was identical to *Schedule 1 and Schedule 2*.

*Schedule 4* was somewhat milder, particularly after the average MC reached 30 % (*Table 5*). The TG was set to rise from 3,3 at the beginning of the schedule to 3,9 at the MC of 30 %, and

then to decrease gradually to 2 at the end of drying. Initial dry-bulb temperature increase rate was changed from 3 min/°C to 5 min/°C.

**Table 5. Drying schedule used for the fourth batch.**

Moisture content (%)	Dry-bulb temperature (°C)	Equilibrium MC (%)	TG (Trocknungsgefälle)
80	68	9	3,3
60	70	8,8	3,4
45	70	8,2	3,7
30	70	7,7	3,9
22	71	7,5	2,9
18	71	7,1	2,5
13	71	6,5	2,0

## 4.2.2 Moisture measurements and moisture profiles

Two different methods were used for moisture content (MC) measuring - resistance and gravimetric. They were conducted according to ÖNORM EN 13183-1 and 13183-2. Afterwards, a comparison between the two methods was performed, as well as an analysis of drying of both glued and non-glued timbers. Additional specimens were extracted from particular glued timbers, later referred to as follow up glued timbers, in order to get a more complete insight into the manner in which glue-layers affect moisture movement through wood, especially in the tangential direction.

### 4.2.2.1 Resistance method

Both kilns were equipped with a system for moisture content measuring, based on the resistance method. This is essentially a non-destructive method, whereby the electrical resistance of wood is measured and its moisture content (MC) calculated from the relationship between the logarithm of MC and the logarithm of electrical resistance in wood (Hartley & Marchant 1995; Skaar 1988; ÖNORM EN 13183-2). The measuring was performed during drying at intervals of 15 minutes, inside the chamber. The effect of temperature and wood species on measurements was taken into account (Kolin 2000). The MC was measured simultaneously on 8 drying units in the first three runs and on 7 pieces in the fourth. The mean value of these measurements was used to control each drying schedule.

Two 5 cm long screws per measuring point were used as electrodes. They were screwed into the wood centrally from the upper face toward the middle of the timber, perpendicular to the grain, meanwhile the distance between the electrodes was kept consistent. In case of glued units, the measuring points were slightly off from the center of the specimen to avoid contact with the glue layer. Furthermore, slices made of rubber were used to prevent contact between possible free water on the wood surface and the electrode (Hartley & Marchant 1995).

### 4.2.2.2 Gravimetric method and moisture profiles

Besides resistance measurements, which were taken rather continuously, the stepwise gravimetric determination of MC was also conducted (ÖNORM EN 13183-1). This method, although destructive and time consuming, would generally be considered the most accurate. It is commonly used for determination of higher levels of MC and as a reference method for validation of the resistance method (Teischinger & Vanek 1987). However, there are several disadvantages associated with this method: inaccurate results for species with significant amount of volatile constituents other than water; increase or decrease in MC during manipulation before weighing – especially for thin specimens; decrease in MC caused by friction during specimen making; shifts from zero of the relative vapor pressure inside the oven; possible effect of sorption history. (Teischinger & Vanek 1987; Skaar 1988)

In the case of this study, the drawbacks mentioned above were attenuated or not significant, hence sufficiently achieved accuracy could be assumed. Both average MC and moisture distribution within the sample were examined. In each run two timbers were chosen, one glued and another non-glued, briefly being removed from the kiln at intervals during drying, in order to take a moisture specimen (*Specimen 1*; *Figure 4.4*). These timbers were labeled as follow up timbers (from which specimens were extracted).

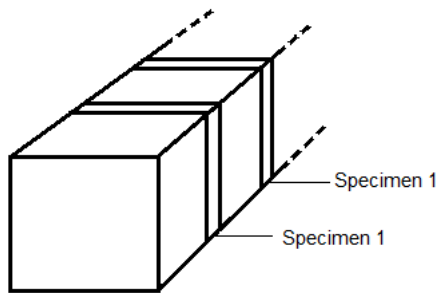


**Figure 4.4.** A follow-up timber for further analysis.

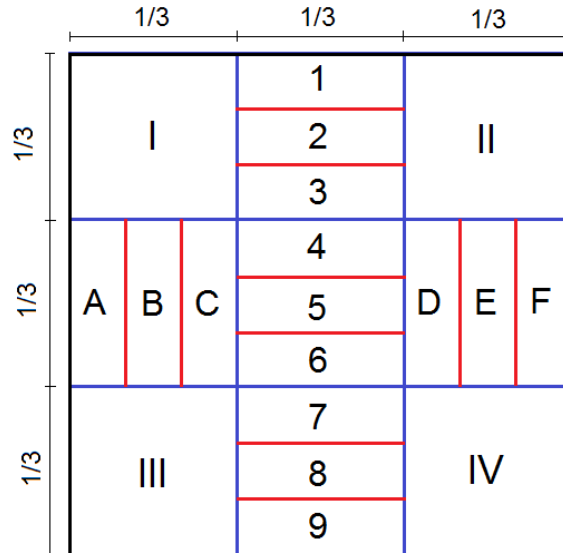


**Figure 4.5.** *Specimen 1* – moisture gradient assessment.

Six such specimens (*Figure 4.4*; *Figure 4.5*) were taken at intervals from each observing timber during *Schedule 1*, with the intervals being 2 to 3 days from the beginning to the end of drying. During subsequent three drying schedules, only four measurements per run were carried out, with intervals of 4 to 5 days. This was due to the lower length of timbers (0,5 m). To avoid the influence of a more rapid drying from the cross-section, *Specimen 1* was taken 15 cm from the front side of timber in the first run and 10 cm from the front side in the remaining three runs.

Outer dimensions of *Specimen 1* were as follows: width and height were that of the drying unit (timber) and thickness was 2 cm in grain direction. Further breakdown of the specimen into smaller segments was done according to *Figure 4.5*, whereby blue lines represent the cut with a bandsaw and the red ones with a chisel. The latter was used to reduce the drying caused by friction (Teischinger & Vanek 1987). Segments were weighed right after splitting, and subsequently dried in an oven at  $103 \pm 2$  °C until constant weight was reached. They were then weighed once again, and the moisture content was evaluated from:

$$MC = \frac{w_m - w_0}{w_0} \cdot 100, \quad (3)$$

where  $w_m$  is the weight of moist and  $w_0$  weight of dry wood. Along with timbers chosen for stepwise measuring, average MC was evaluated for all other drying units after each drying schedule.

Moisture distribution was, however, determined on a specific number of timbers. After the first run it was carried out on 8 timbers (four non-glued and four glued), and after each following run on 4 timbers (one non-glued and three glued). These measurements were also performed in the conditioning phase (*Chapter 4.2.3*).

Other than the “standard” cutting pattern for evaluating moisture distribution mentioned above (*Specimen 1*), two additional patterns were used during Schedules 2,3 and 4 (*Figure 5.22*; *Figure 5.23*). *Figure 5.22* depicts specimen used during the second and third run (*Specimen 2*), and *Figure 5.23* refers to the specimen used during the fourth run (*Specimen 3*). These additional patterns had the purpose to shed light on whether glue layers represented a

significant barrier for moisture movement from the central part toward outer zones of the drying unit.

For this purpose, one additional follow up timber per schedule was chosen. Procedures of extraction from the drying unit and evaluation were equivalent to those of *Specimen 1*.

### 4.2.3 Conditioning

After schedules 2, 3 and 4 conditioning was carried out in a room with a controlled climate. Temperature and relative humidity were set to 20 °C and 65 % respectively, hence the equilibrium MC was around 12 %. The conditioning phase lasted 15 days after the second and third schedule, and 5 days after the fourth. In the former case, two measurements of moisture distribution and average MC were taken, during and after the 15-day conditioning, while in the latter case only one measuring took place, after the 5-day conditioning. Average MC was examined on all timbers and moisture distribution evaluation was performed on the same drying units used at the end of the kiln-drying schedule (*Chapter 4.2.2.2*).

### 4.2.4 Twist and bow

Twist, a spiral distortion along the length of the specimen, was examined during *Schedule 1* on all pieces except the follow-up timbers. A three-point measuring was conducted. The measuring device was made of a thick plywood plate, with four dowels in it, placed perpendicularly to the board plain (*Figure 4.6*). Dowels were fixed into the board in such a way that they formed a rectangle with the longer sides equaling 100 cm and shorter ones equaling 11,5 cm. All dowels were of the same height. Timbers were centrally placed onto the device, and the distance between the tip of the dowel and the part of the drying unit not touching the device was measured with a caliper. Five measurements were taken in total, four of which were performed at intervals during drying on a sample of ten timbers, five non-glued and five glued. The fifth and final measuring was done at the end of the drying schedule on all units, except for follow-up units used for moisture measuring.



**Figure 4.6. Three-point measuring device for twist deformation assessment.**

Bow, a deviation in longitudinal direction of the drying unit, which causes the face to curve away from its intended plain, was measured only after the first run. It was evaluated along 1 m of 1,5 m long timber (*Figure 4.7*). The measuring was done on two bowing sides of each specimen, not including follow-up samples.

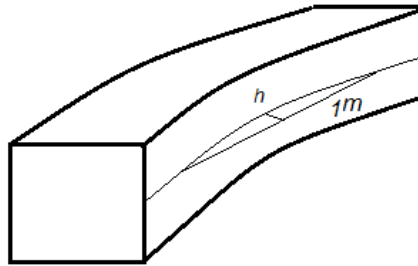


**Figure 4.7. Bow deformation measuring ( $h$  – pitch along 1m length).**

#### 4.2.5 Case-hardening

In order to carry out the assessment of case-hardening, a modified method from the ÖNORM ENV 14464 standard was employed. Specimens of the same outer dimensions as *Specimen 1*, used for moisture measuring, were cut out of the follow-up timbers and then split in half with a band saw after each drying schedule. The measuring was carried out 24 to 36 hours after each drying schedule. In the case of specimens of the fourth batch, an additional measurement was taken after 5-day conditioning in a room with a controlled climate. Samples were placed onto the specimen holder (*Figure 4.8*), and the distance in the middle was measured with a calibrated caliper. In order to get the case-hardening, the diameter of the cylinder on the specimen holder, which was 10 mm, was subtracted from the measured distance.

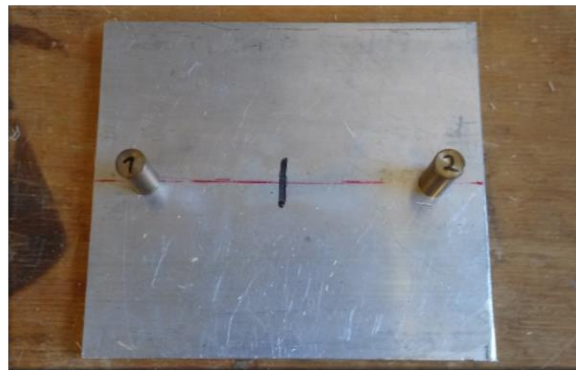


**Figure 4.8. A device for case-hardening evaluation (according to ÖNORM ENV 14464).**

#### 4.2.6 Cross-section scanning and material loss assessment

Having in mind that timbers at *Stora Enso* are planed after drying in order to get a product with a rectangular cross-section, every deformation during drying represents a loss of material. In order to see whether glued timbers provide a more efficient material use, deviation from a rectangular cross-section was evaluated for every drying unit after each drying schedule. For that purpose, specimens were scanned in high resolution, having corresponding cross-sections to the drying units and a thickness of 2 cm in grain direction (*Figure 5.32*; *Figure 5.33*). Afterwards, images were scaled in Auto-CAD, and the loss of material due to deformation calculated. The area of irregularly shaped deformation was computed in Auto-CAD. The loss of material was calculated as follows:

$$L_{deformation} = \frac{A_{deformation}}{A_{dry}} \cdot 100 (\%) \quad (4)$$

where  $L_{deformation}$  is the loss of material due to deformation of the cross-section,  $A_{deformation}$  represents the area of irregularly shaped deformation, and  $A_{dry}$  is the area of the rectangular cross-section of a timber after drying.

It should be noted that twist and bow deformations were not taken into account.

#### **4.2.7 Checks**

All checks were evaluated by their length after each schedule and sorted in different categories. The measuring was conducted with a tape measure. It was distinguished between surface and end-checks. End-checks were those recorded on two fronts, cross-sectional sides, and all other checks, recorded on the remaining four faces, were labeled as surface checks. In order to draw a comparison between non-glued and glued timbers, surface checks were further categorized according to the side of their occurrence and type of the check – pith/knot checks; checks not reaching the front; checks reaching the front.

Furthermore, all checks were counted and classified by a length category. End-checks were arranged in three length categories: 0-2 cm; 2-5 cm; and 5-15 cm. On the other hand, surface checks were sorted in four length classes: 0-2 cm; 2-5 cm; 5-20 cm; and >20 cm.

The width of checks was measured only on a small portion of the population, just to get a rough comparison between non-glued and glued timbers. The measuring was performed with a calibrated caliper.

# 5 Results

## 5.1 Parameters for drying

The drying time of the different test runs is summarized in Table 6. It took from 254 to 283 hours to dry the timber pieces to a mean moisture content of 15 % (resistance method). The drying time decreased with every following drying schedule. This was not as anticipated, since the intensity of drying schedules decreased over the entire study. However, differences between drying schedules were relatively small (*Chapters 4.2.1.1 and 4.2.1.2*) and the discrepancy of the measured average MC between *Schedule 4* and the remaining three runs was only up to 2 % after 254 hours of drying.

**Table 6. Drying duration. Schedules 1-4.**

	Drying time (h)	Kiln
Schedule 1	283	Mühlböck
Schedule 2	274	Vanicek
Schedule 3	266	Vanicek
Schedule 4	254	Vanicek

The actual drying parameters were close to the parameters set in the program (*Chapters 4.2.1.1 and 4.2.1.2; Figure 5.1; Figure 5.2*) over the course of all drying schedules. One exception was at the beginning of *Schedule 1*, when a problem with the moistening system occurred. As a result, the ratio of actual MC to equilibrium MC ratio (*Tg*) rose gradually from 4,5 to 7 in the second 10 hours of drying. It could be assumed that this led to increased moisture gradients (*Chapter 5.2.3*), thus prolonging this particular drying schedule compared to the remaining three (*Chapter 6.2*).

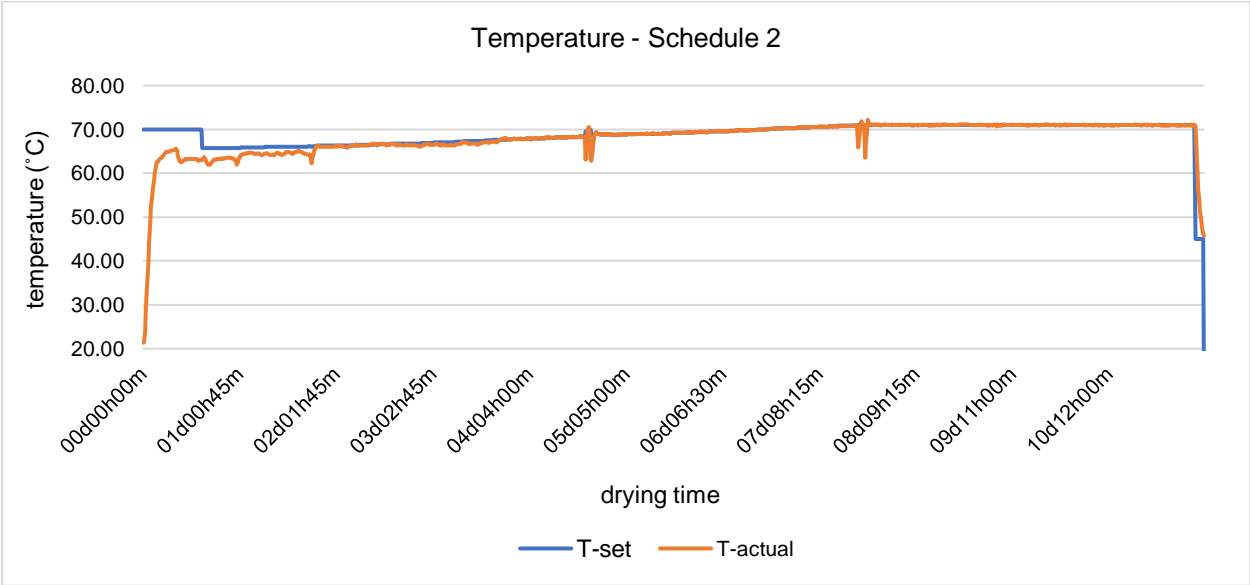


**Figure 5.1. Temperature trend - Schedule 2.**

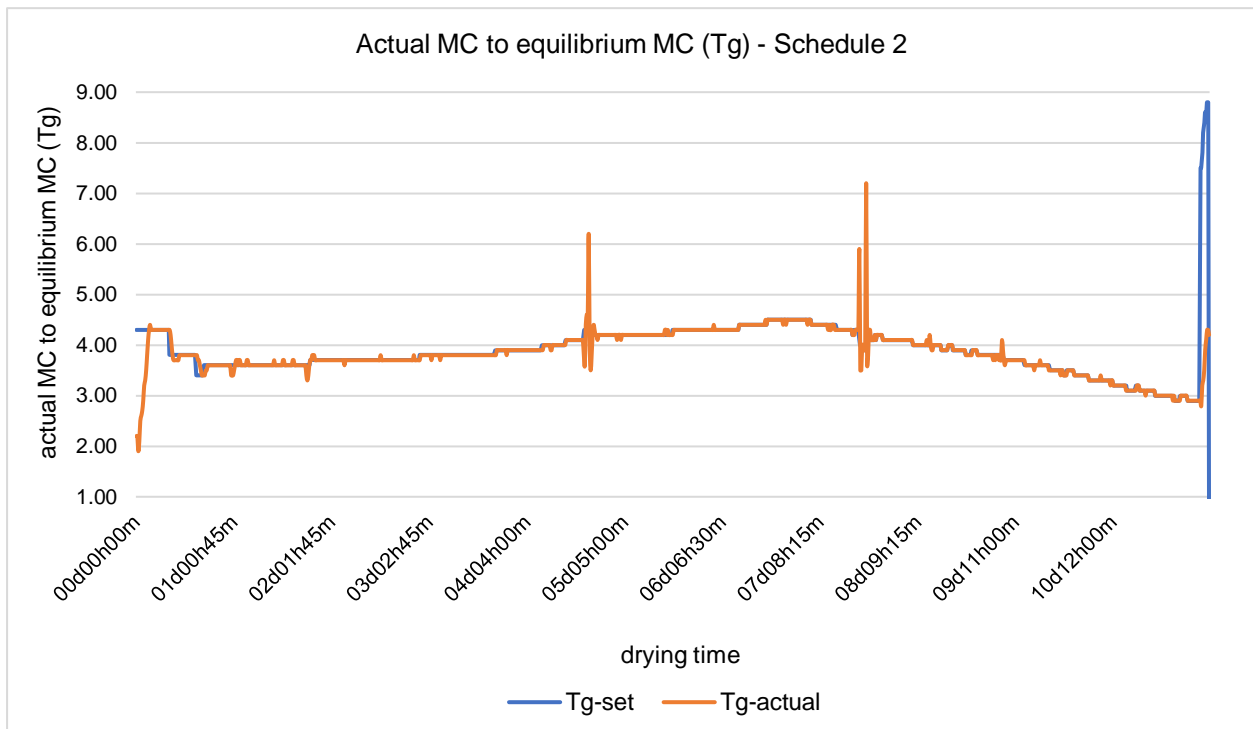


**Figure 5.2. Actual moisture content to equilibrium moisture content (Tg) – Schedule 2.**

The actual temperature was a few degrees Celsius lower than the set-value during the first two days of *Schedule 2*, but remained consistent for the rest of the program (*Figure 5.1*). In the remaining cases, there was nearly no discrepancy between set and actual temperatures. Two peaks during day 5 and day 8 of drying, in both *Figure 5.1* and *Figure 5.2*, occurred due to the kiln door opening for additional measurements.

## 5.2 Moisture content

Characterizing the drying process, surprisingly, no major variation in drying rates was noticed between glued and non-glued units. As well, relatively mild changes in drying schedules did not significantly affect the drying rate. However, the influence of initial moisture content as well as wood density was considerable. Moreover, vast discrepancy between the gravimetric and resistant measuring method was recorded. This issue is thoroughly discussed in chapters 5.2.1.2 and 6.4.

### 5.2.1 Drying trends

*Figure 5.5* shows drying trends of follow-up timbers (*Schedules 2 to 4*). The lines illustrate results of measurements based on the resistance method, while dots represent those based on the gravimetric method, measured on *Specimen 1* (average moisture content; *Figure 5.3*). In order to facilitate comparison, each color represents one single drying schedule. Dark color is for glued units and light color for non-glued timbers. *Schedule 1* is not included in the comparison of drying trends (*Chapter 6.2*).

Firstly, the gravimetric method is analyzed and later the resistance method.

#### 5.2.1.1 The gravimetric method

*Specimen 1* (*Figure 5.3*) was used for this analysis. Specimens labeled with light green, dark green and light blue dots dried in a similar fashion. These timbers had very close initial MC, around 35 %, and similar basic density. No significant difference in drying rate between glued and non-glued timber units was detected, which is expressed in *Figure 5.5*.

Specimens of glued timber 70B – run 2G from the second batch (dark blue dot) had a higher average initial MC than those of non-glued timber N4 – run 2G from the second batch (light blue dot); 47,5 % and 35 % respectively. Nevertheless, it took the same amount of time to dry them to nearly equivalent end moisture content. However, the moisture distribution was different between the two timbers. The share of free water in this glued unit was much higher than in non-glued one. In the periphery area it varied from 70 % to 100 % compared to 35 % for non-glued unit. In contrast, the amount of free water in the middle of the piece was 10 % higher for the non-glued timber, amounting to 40 % as compared to 30 % for the glued piece. The capillary water from outer parts (sapwood) dried much faster than free water from central, heartwood, zone (Chapter 6.2, Figure 5.6; Figure 5.7; Figure 5.11). Such a trend was recorded in all other examined pieces as well. Furthermore, the much slower drying of bound water from the central zone of both non-glued and glued timbers compared to outer parts was observed (Figure 5.6; Figure 5.7). Therefore, much faster capillary movement from the outer parts of glued timber compensated the higher moisture content.

Non-glued specimens of timber N3 – run 3G (light orange dots) dried more quickly than glued 39B – run 3G (dark orange dots), most likely due to lower density. The annual rings of light orange specimen were almost twice as wide as those of dark orange.

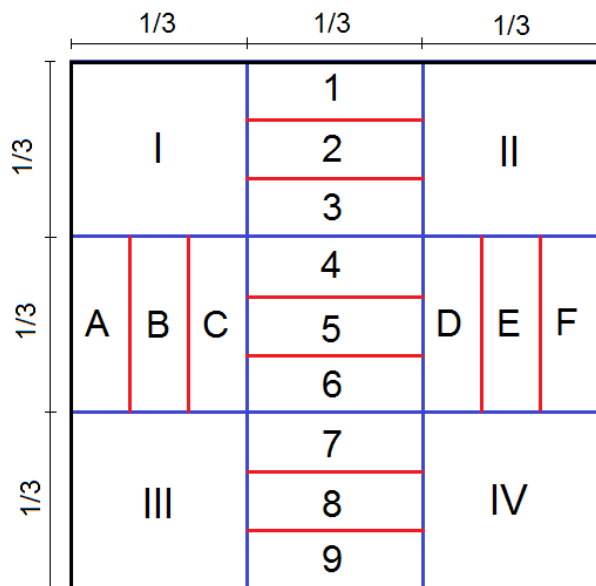
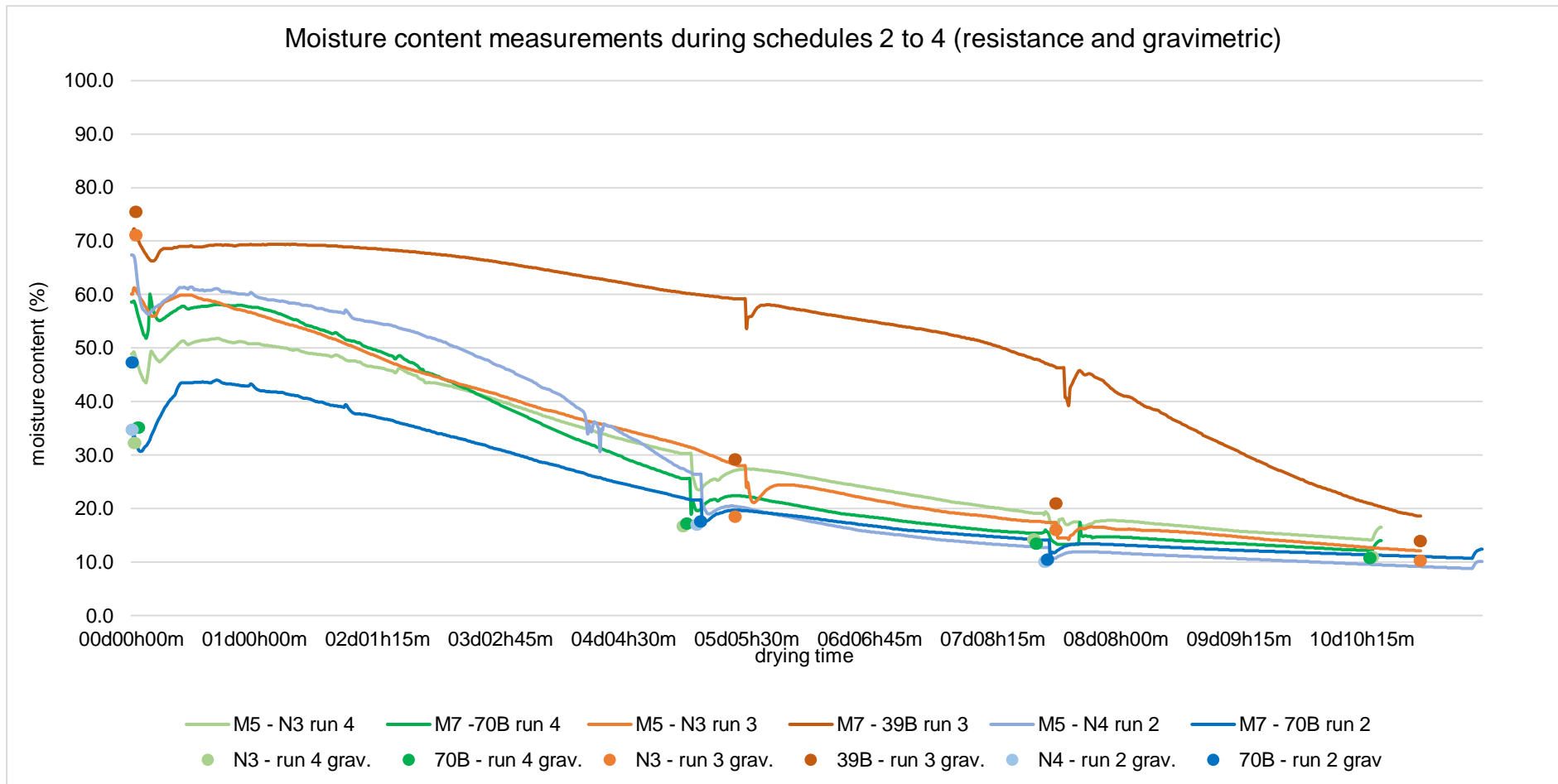


Figure 5.3. Specimen 1 – A specimen used for moisture content and moisture distribution assessment.



Figure 5.4. Cross-section of a glued timber in "green" state.



**Figure 5.5. Moisture content measurements during schedules 2 to 4 (resistance “-” and gravimetric “grav.” methods).**

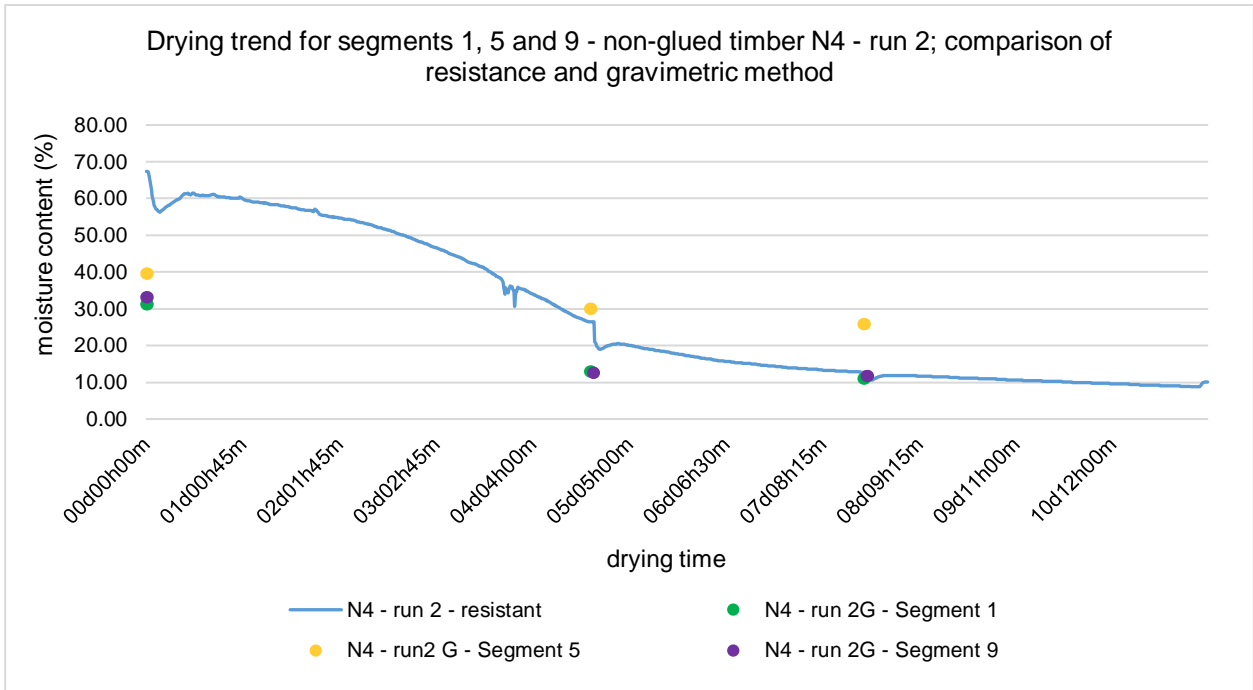


Figure 5.6. Drying trend for segments 1, 5 and 9; non-glued timber N4 - run 2; comparison of resistance (line) and gravimetric (dots) method.

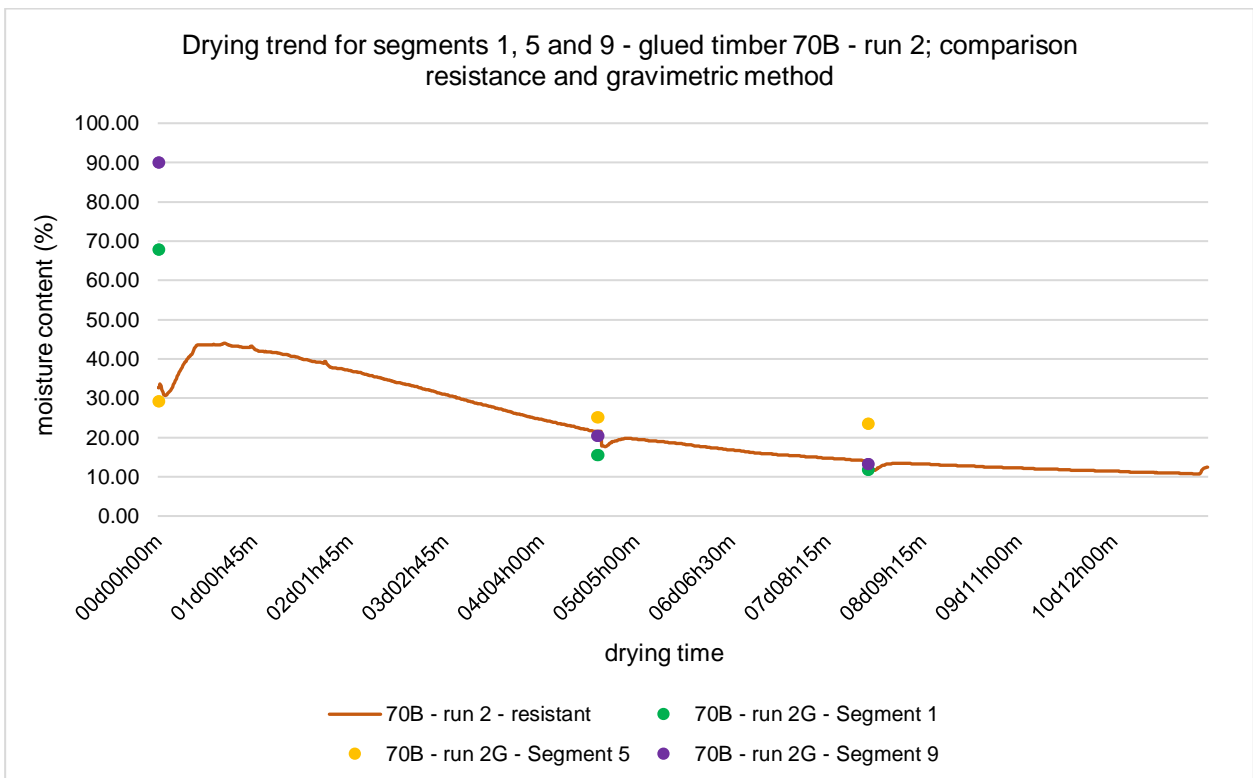


Figure 5.7. Drying trend for segments 1, 5 and 9; glued timber 70B - run 2; comparison of resistance (line) and gravimetric (dots) method

### 5.2.1.2 Resistance vs gravimetric methods – comparison

Although measuring with the resistance method provides local values of moisture content, these were used, as commonly done in the practice, for controlling the drying schedule. Hence, each of the local values represented the whole corresponding timber (*Chapter 4.2.2.1*). Therefore, these values were compared to the average values recorded using the gravimetric method.

A significant variance between the results of gravimetric (mean values) and resistance method was observed at most of the examined pieces. High inaccuracy of the resistance method was noticed with moisture contents above the saturation point. The discrepancy between two methods rose with an increase in maximum moisture content in a single drying piece. Other than moisture content, moisture distribution within a single timber has a considerable influence on the variation between two methods. To make a better and more accurate comparison, both methods were conducted on the same timbers in schedules 2, 3 and 4. Therefore, one color - a dot for gravimetric and a line for resistance method - represent measurements on one single timber (*Figure 5.5*).

The discrepancy was the highest at the beginning of drying process for timbers with relatively low average initial moisture content, which was around 35 %. Light blue, light green and dark green lines in *Figure 5.5* indicate that. However, relatively high moisture content, from 45 % to 80 % was recorded, on the periphery of the cross-section in local zones, where resistance measuring was performed.

Timbers with higher initial moisture content showed the highest variance after five days of drying. At this point periphery of the timber dried considerably. Extreme results (resistance method) were recorded for timbers in which high amount of sapwood free water stretched to deeper zones (segments 7 and 3 from *Specimen 1*; *Figure 5.3*; *Figure 5.4*). All observed timbers with maximal measured moisture of over 130 % displayed such a trend (*Figure 5.8*). This caused over-drying of almost all timbers at the end of each schedule. As it can be seen in the figure, all timbers had labels 39 or 46, meaning that they were sawn from the same stem. Such labeling applied only to glued timbers. Dark orange dots represent measurements with a reference, gravimetric method.

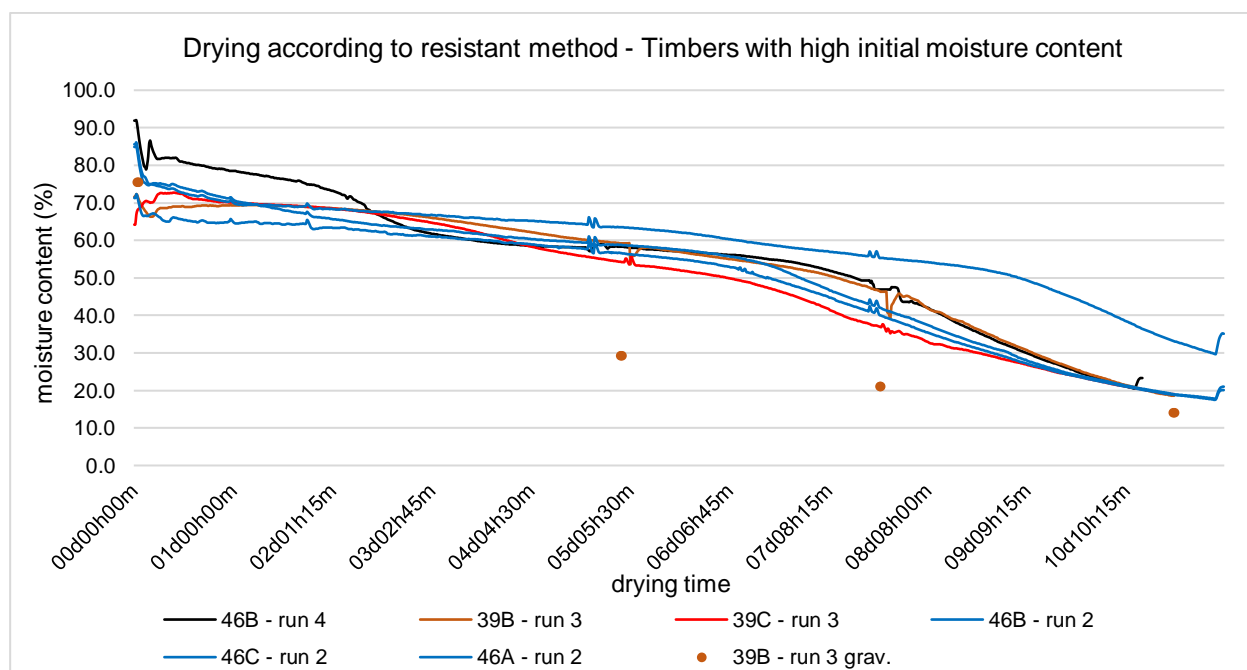


**Figure 5.8. Drying according to resistance method - Timbers with high initial moisture content. (resistant – lines; gravimetric – dots).**

## 5.2.2 Average moisture content at the end of drying

Measurements of the average moisture content were done on all timbers at the end of every drying schedule. The quartiles for non-glued and glued timbers are plotted in *Figure 5.9* and *Figure 5.10* respectively.

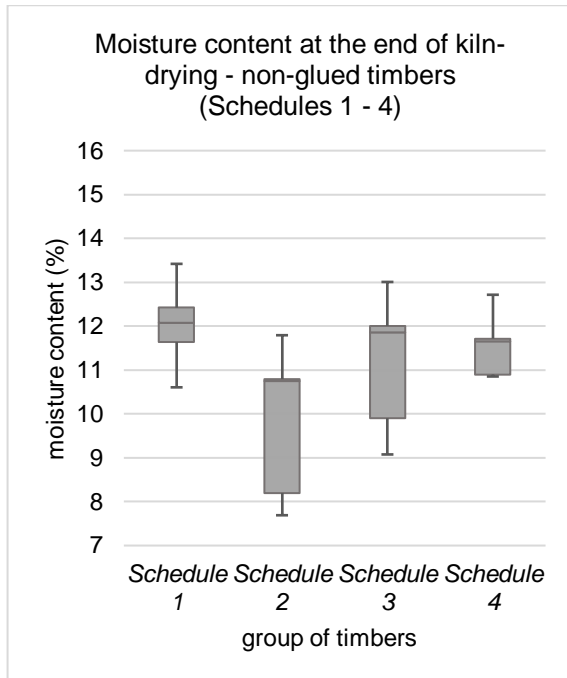


**Figure 5.9.** Moisture content at the end of kiln-drying - non-glued timbers (Schedules 1 - 4).

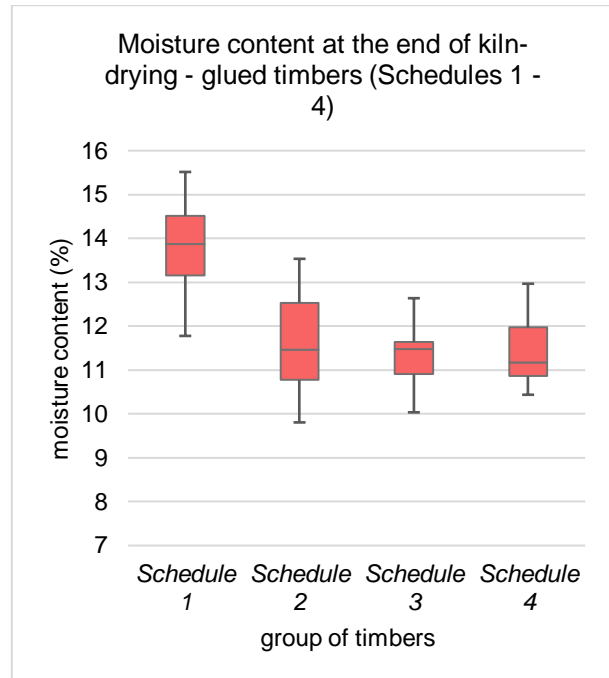


**Figure 5.10.** Moisture content at the end of kiln-drying - glued timbers (Schedules 1 - 4).

Distinctively higher values were recorded at the end of the first schedule, especially for glued timbers, due to reasons discussed in *Chapter 6.2*. However, almost all timbers were over-dried as a result of unrepresentative measurements of the resistance method. The target MC was set to 15 %. The non-glued units from the second batch dried to very low moisture contents owing to very low initial MC. In contrast, so much as three glued timbers with very high initial MC were used for controlling this particular drying program (*Figure 5.8*, blue lines). This was probably the main reason for prolonged drying time compared to schedules 3 and 4. The timbers from third and fourth batch, both glued and non-glued, dried to similar levels.

## 5.2.3 Moisture distribution and moisture gradients

Initial moisture distribution was differently shaped for glued and non-glued timbers, due to specific structure of the glued pieces. Moisture distribution of non-glued timbers depended mostly on their earlier position in the stem, and therefore varied significantly from one piece to another. In contrast, moisture distribution of glued units had quite a homogenous pattern. Sapwood was always positioned on two opposite tangential sides of the timber (*Figure 5.4*). Therefore, the initial MC was, if in green state, much higher on these two sides than on the radial ones.

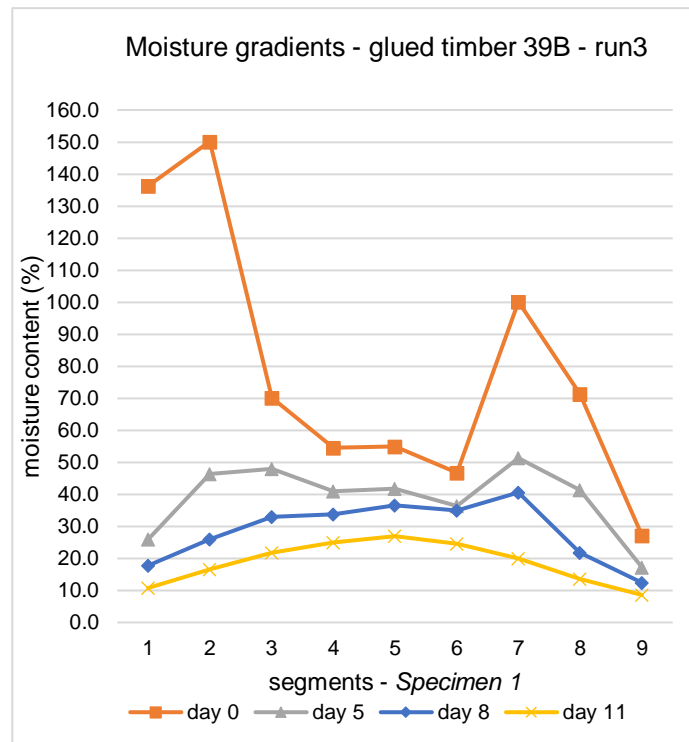


**Figure 5.11. Moisture gradients evaluated at intervals from the beginning to the end of drying - glued timber 39B – run 3.**

A typical moisture distribution for glued timbers in “green” state is shown in *Figure 5.11*, measured from *Specimen 1* (*Figure 5.3*). Additionally, the gradients during subsequent drying are also illustrated. High amounts of free water were measured up to the second third of the specimen, looking centrally from the tangential side. In *Figure 5.11* it is obvious that free water from the deeper *Segment 7* moved much slower toward the surface than from the closer *Segment 2* (*Chapter 6.2*). Even after 8 days of drying *Segment 7* was above saturation point, which caused, as discussed in *Chapter 6.4*, such high MC values measured with resistance method. By contrast, MC of segments 1 to 4 in the corners of the cross-section varied from 10 to 13,5 % at the same time.

Very slow drying in the middle zone of timbers (segments 4, 5 and 6) was measured for both free and bound water. Such results were recorded on all observed timbers, independent of their type (*Chapter 6.2*). Consequently, timbers with a considerable initial MC in the middle zone (*Figure 5.11*; *Figure 5.4*) exhibited a significant moisture gradient at the end of a drying schedule.

In order to compare drying trends of non-glued and glued timbers, two pieces with alike density as well as comparable initial MC and moisture distribution were chosen (*Figure 5.12*; *Figure 5.13*). Very similar, quite homogenous, gradients were measured, indicating that both capillary and bound water moved towards the surface without major difficulties caused by glue layers. Capillary water from segments 8 and 9 moved rapidly to the evaporating front, and diffusion rate was similar to that of the non-glued timber.

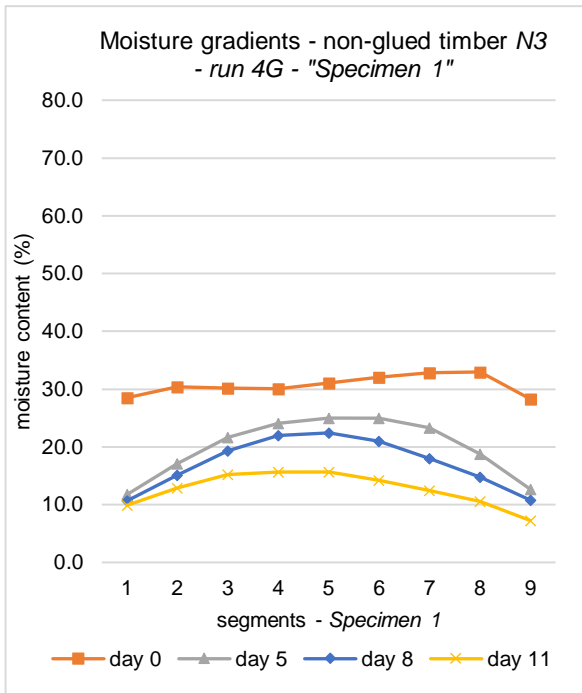


**Figure 5.12. Moisture gradients evaluated at intervals from the beginning to the end of drying - non-glued timber N3 - run 4G - "Specimen 1".**

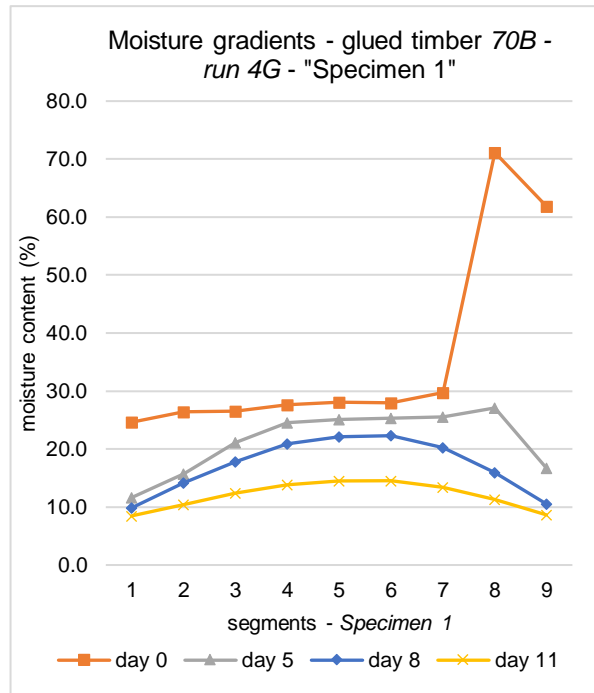


**Figure 5.13. Moisture gradients evaluated at intervals from the beginning to the end of drying - glued timber 70B - run 4G - "Specimen 1".**

Additional evaluations of moisture gradients were done at the end of each drying schedule. No notable difference between schedules 2, 3 and 4 was identified. However, the origin of timbers, and consequently their initial MC and density, were the determining factors for variation of moisture gradients. To illustrate this point, moisture gradients of observed timbers at the end of schedules 2, 3 and 4 are depicted in *Figure 5.14*, with each color representing one single schedule. On the other hand, gradients are colored by their origin in *Figure 5.15*, with each color representing a single stem of which the timbers were made. Non-glued timbers are in both *Figure 5.14* and *Figure 5.15* represented as a separate group, since their origin was unknown and there was no significant scattering between them. Timbers from stems 46 and 39, with average and maximum moisture content starting from 75 % and 130% respectively, clearly distinguished themselves from the rest in the higher half of the diagram. In contrast, timbers cut from stems 11, 50 and 70, with an average and maximum moisture content up to 60 % and 100 % respectively, had gradients much more similar to those of non-glued pieces.

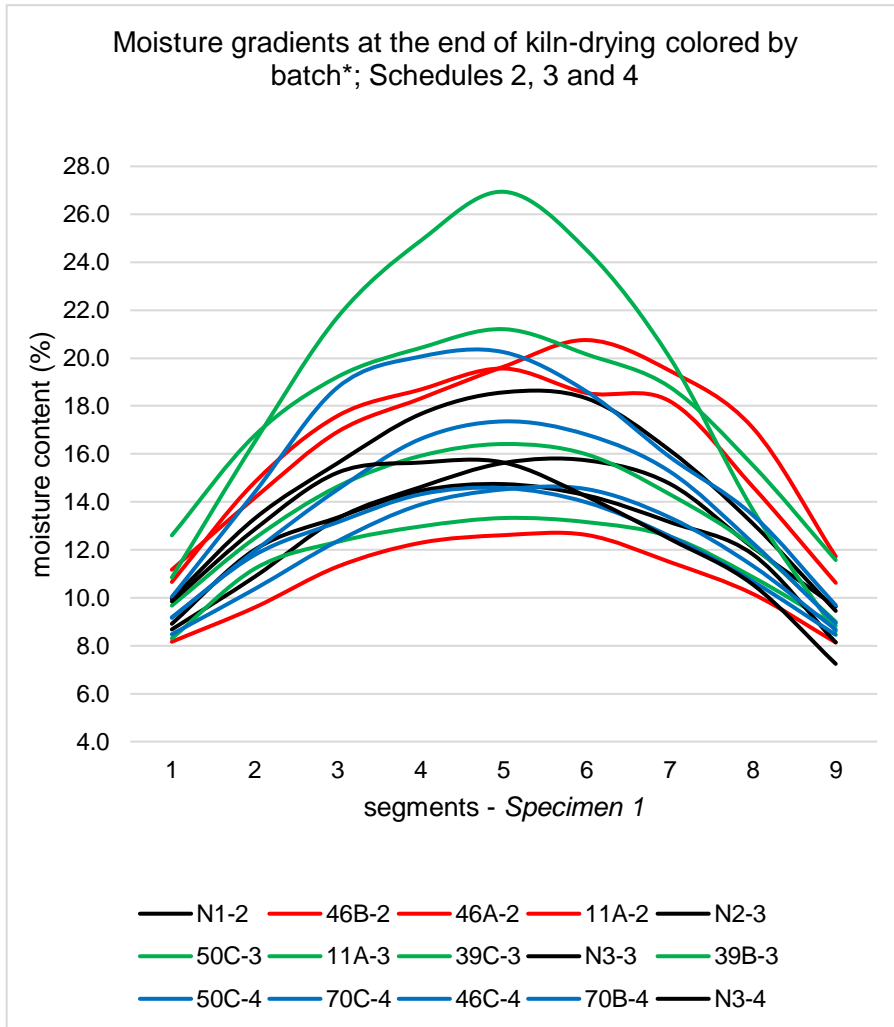


**Figure 5.14. Moisture gradients at the end of kiln-drying colored by batch\*;** Schedules 2, 3 and 4.  
 \*each color represents one drying schedule (glued timbers); exception - black lines represent non-glued timbers regardless of the batch number.

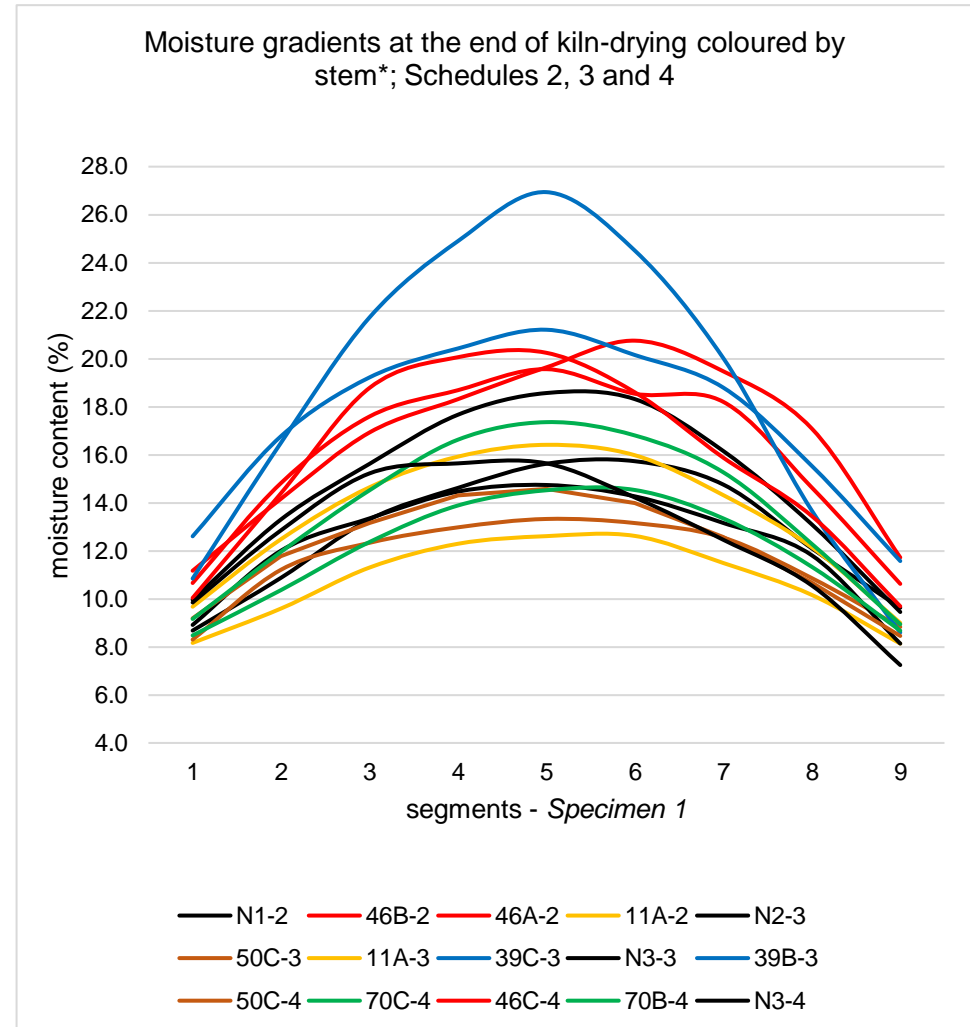


**Figure 5.15. Moisture gradients at the end of kiln-drying colored by stem\*;** Schedules 2, 3 and 4.  
 \*each color represents a stem from which the timbers are sawn (glued timbers); exception – black lines represent non-glued timbers regardless of the origin.

In order to compare non-glued and glued timbers, their minimum, mean and maximum moisture contents per segment are separately plotted in *Figure 5.16* and *Figure 5.17*. The values of segments 1 to 9 of *Specimen 1* at the end of the kiln-drying schedules 2, 3 and 4 are illustrated. Average moisture contents were close, having in mind the dimensions of lumber. The results showed, however, a much higher range between minimum and maximum values for glued units.

*Schedule 1* was not included in diagrams below, due to a very harsh first day of drying, which most likely influenced the moisture gradients. The values in the middle segments at the end of drying varied from 22 % to 29 % for glued timbers, while the MC in the surface zones was around 11 %. This was mainly because all observed timbers originated from stems 46 and 39, which had the highest initial MC. In addition, the high *TG* at the beginning of drying also could have made a contribution to such measurements.

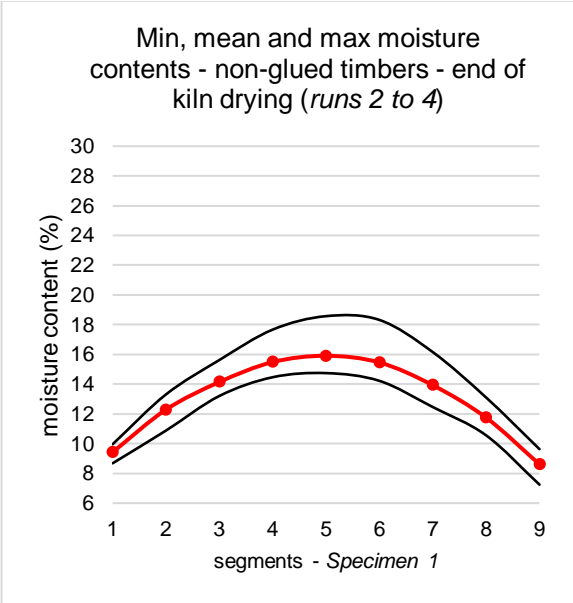


**Figure 5.16.** Min, mean and max moisture contents - non-glued timbers - end of kiln drying (runs 2 to 4).

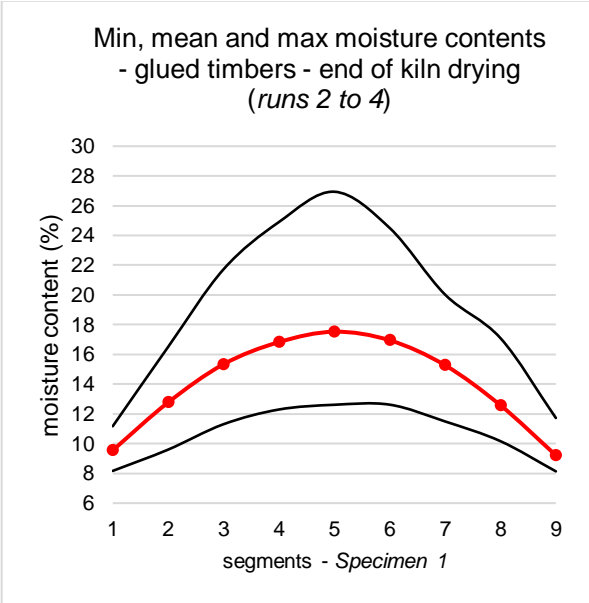


**Figure 5.17.** Min, mean and max moisture contents - glued timbers - end of kiln drying (runs 2 to 4).

After 15 days of conditioning in a controlled climate, at 12 % equilibrium MC, the moisture gradients were mitigated (*Figure 5.18*; *Figure 5.19*). The reduction was, as anticipated, most intense involving timbers with highest gradients at the end of the kiln-drying. The mean moisture content varied from surface zones to the center from 10% to 13,4 % for non-glued, and from 11% to 14,5 % for glued specimens.

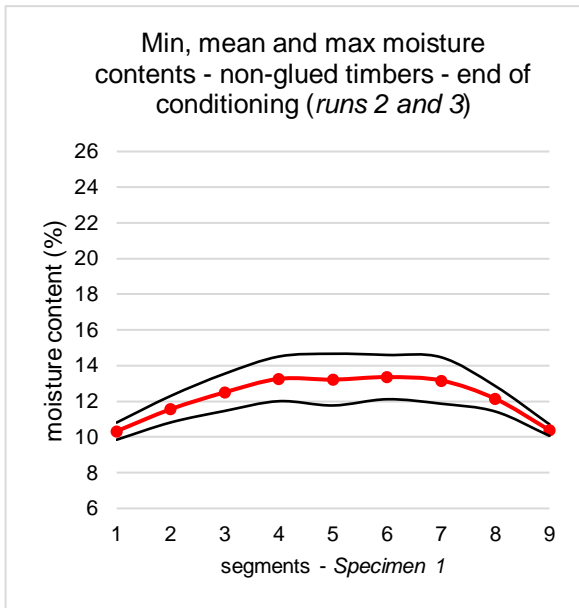


**Figure 5.18. Min, mean and max moisture contents - non-glued timbers - end of conditioning (runs 2 and 3).**

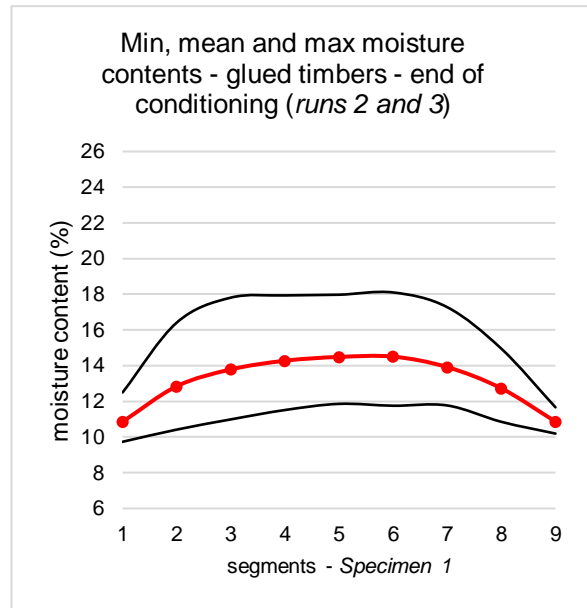


**Figure 5.19. Min, mean and max moisture contents - glued timbers - end of conditioning (runs 2 and 3).**

The gradient in the other, tangential direction (A to F; Specimen 1; Figure 5.3) of glued timbers depended on the initial MC of the segments in sapwood zone (segments 1 to 3 and 7 to 9; Specimen 1; Figure 5.3), given that segments A, B, C and D, E, F were always located in the heartwood area. If MC in sapwood part was great, then there would be a significant moisture gradient in tangential direction after a long period of time. However, if initial MC was equally balanced throughout segments, then moisture gradient during drying would be similar in both radial and tangential directions. In any case, gradients are similar at the end of drying. Figure 5.20 and Figure 5.21 illustrate moisture gradients during drying of non-glued and glued units, with similar initial MC and density, in tangential direction (compare Figure 5.20 and Figure 5.21 with Figure 5.12 and Figure 5.13).

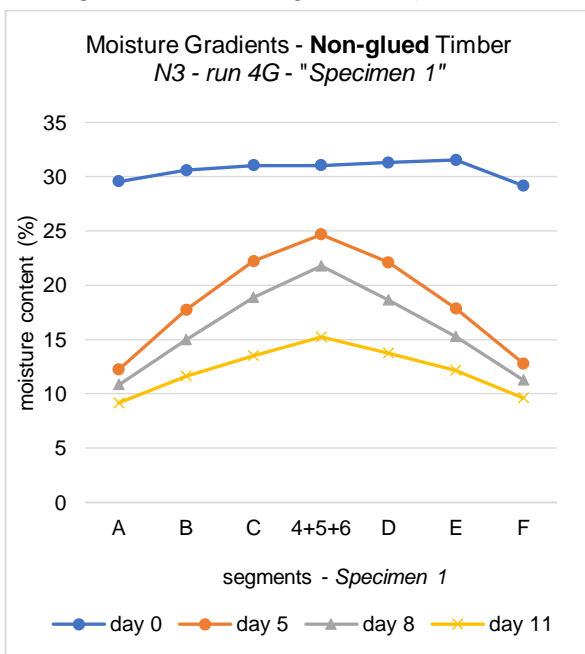


**Figure 5.20. Moisture gradients from the beginning to the end of drying - non-glued timber N3 - run 4G - "Specimen 1".**

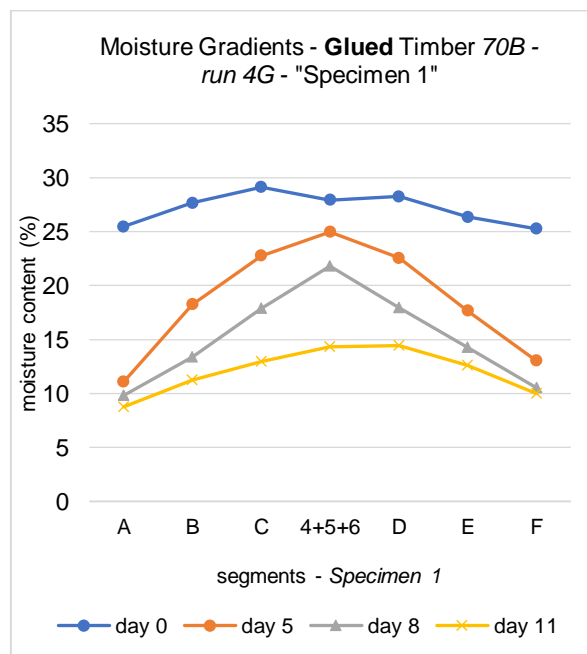


**Figure 5.21. Moisture gradients from the beginning to the end of drying - glued timber 70B - run 4G - "Specimen 1".**

### 5.2.4 Specimens 2 and 3

Specimens 2 and 3 were created in order to examine whether there would be a significant effect of a glue layer on the drying rate of timbers.

According to *Specimen 2* (Figure 5.22) no major influence of gluing layers on the drying process was detected. The middle segments of a drying unit had a higher moisture content regardless of glue lines.

*Specimen 3* (Figure 5.23) was intended to make clear whether narrowing of two neighboring glue layers could affect moisture movement at the narrow side of the corresponding section. Therefore, the opposite segments of a single section were compared (*I* to *III* and *IV* to *II*). The results of the follow-up timber are plotted in Figure 5.25. Each single section is represented by a different color, with a darker color displaying the segment from a wider zone, while a lighter color stands for the segment from the narrow zone. In the first five days of drying the influence of transport mechanism was obvious. Capillary moisture from segments *I* and *IV* moved rapidly toward evaporation front, compared to bound water and vapor diffusion in the segments *II* and *III*. Drying in *I* and *IV* gradually slowed down by increasing the share of diffusion due to pit aspiration (Chapter 2.5). Eventually, all segments had relatively the same moisture content at the end of drying schedule. The influence of glued layers could be seen, although it was not major. Both segments from the wide zone needed three days to dry from around 20 % to 12 %, while segments from the narrow zone needed six days. However, it appeared that with a decrease in moisture content the diffusion coefficient became much more influential than the effect of gluing, since *Segment IV* dried only 1 % in the last three days of the process.



Figure 5.22. Specimen 2

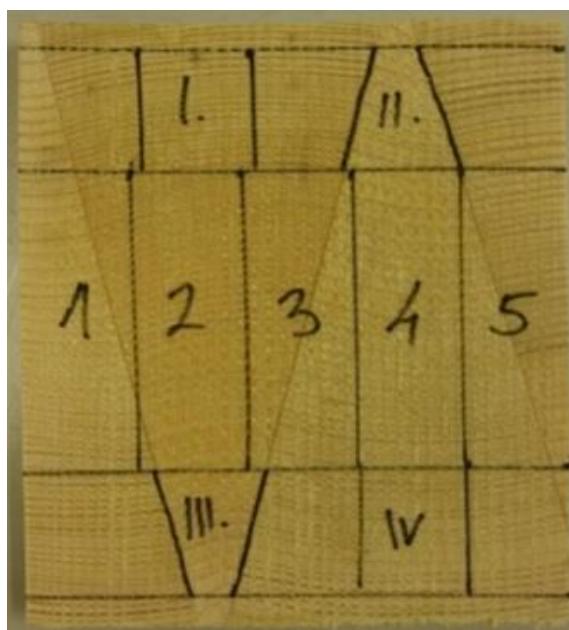
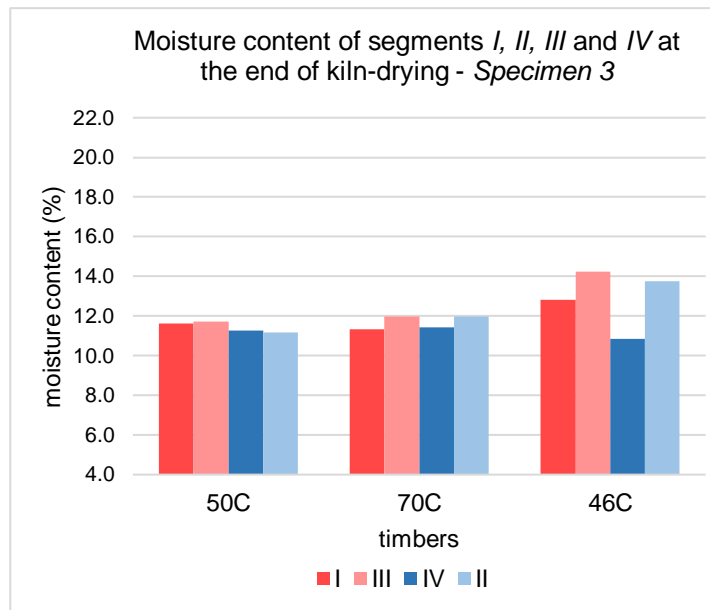


Figure 5.23. Specimen 3

Additional measurements were carried out on three more timbers at the end of fourth drying schedule (Figure 5.24). The difference in MC between the segments of the corresponding section (*I-III*, *IV-II*) varied from -0,1 % to 0,7 % for timbers 50C and 70C, while it was somewhat higher for timber 46C with 1,4 % and 2 %.



**Figure 5.24. Moisture content of segments I, II, III and IV at the end of kiln-drying - Specimen 3.**

The influence of gluing lines on capillary movement was not evaluated, since the narrow side of a single section was always in the region of heartwood, near the pith where no or hardly any capillary movement is present.

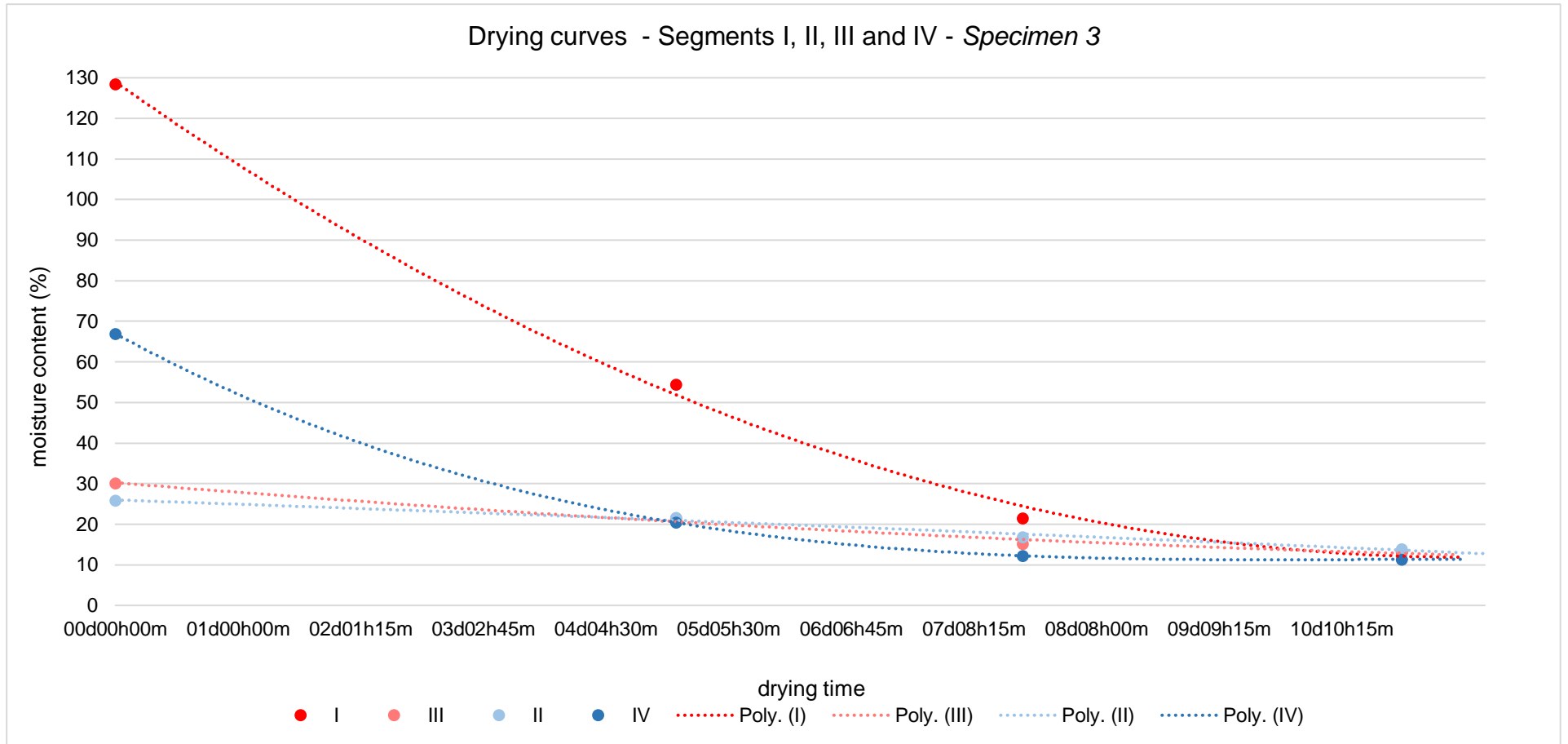


**Figure 5.25. Drying curves - Segments I, II, III and IV - Specimen 3 (dots – gravimetric measurements; dotted lines – polynomial fit).**

### 5.3 Twist and bow

Twist and bow were examined on drying units of the first batch, excluding follow-up timbers used for gravimetric moisture evaluation. The remaining three batches were not included in this analysis due to insufficient length of drying units.

#### 5.3.1 Twist

Twist measurements were conducted at intervals on a sample of 10 timbers; the results are displayed in *Figure 5.26* and *Figure 5.27*.

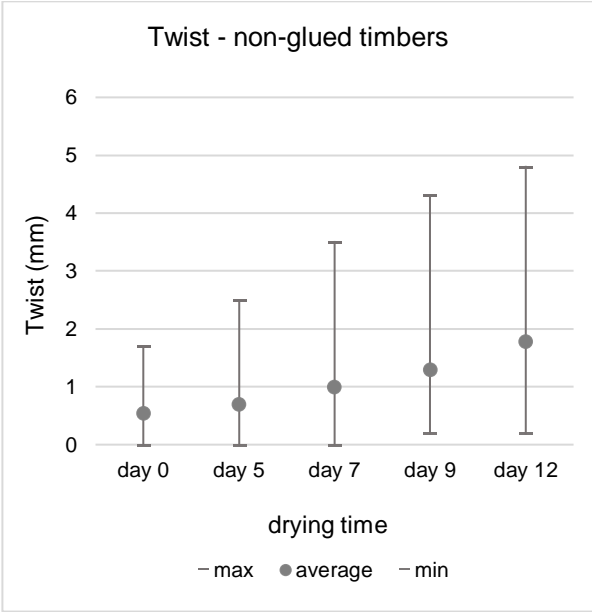


**Figure 5.26. Twist evaluation during drying – non-glued timbers.**



**Figure 5.27. Twist evaluation during drying – glued timbers.**

As it was anticipated, the twist deformation progressed more rapidly in the second half of the drying schedule. A slightly higher average value was recorded for glued timbers of the sample. However, the scattering was much higher in the case of non-glued units.

*Figure 5.28* and *Figure 5.29* display the results recorded at the end of Schedule 1.

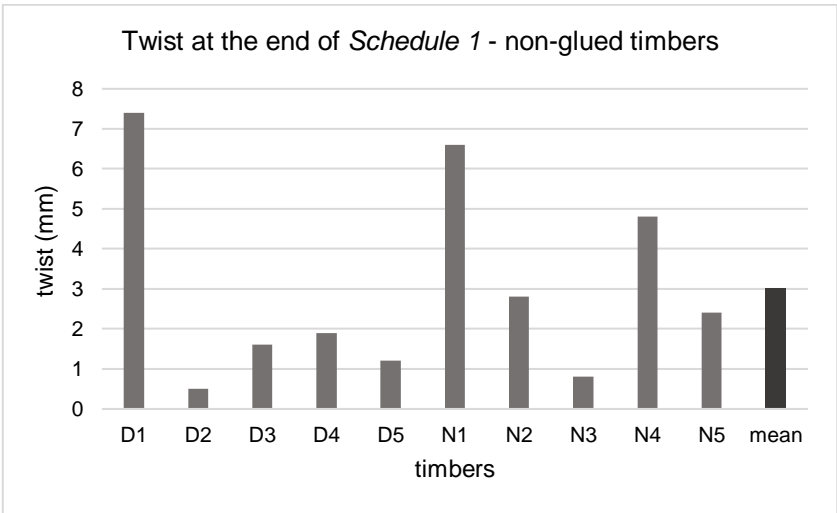


**Figure 5.28. Twist at the end of Schedule 1 - non-glued timbers.**

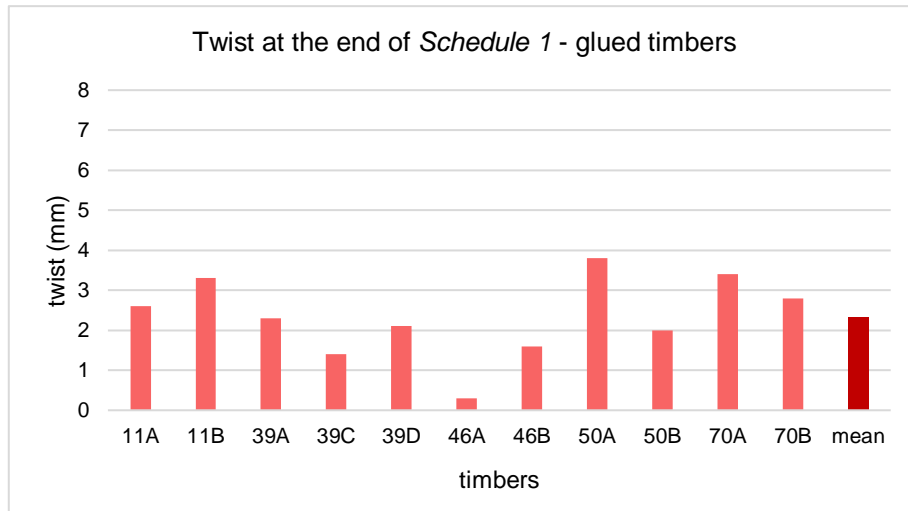


Figure 5.29. Twist at the end of Schedule 1 - glued timbers.

The mean twist of all glued timbers was lower than that of non-glued timbers. While glued drying units deformed quite uniformly around the mean value, non-glued ones behaved rather unevenly, exhibiting either a very low or a quite high twist. This was due to high deformation of units containing the pith.

### 5.3.2 Bow

Bow was negligible for nearly all timbers, both non-glued and glued. Most of the units showed no bowing, with the mean values under 0,5 mm and maximum up to 2,1 mm (Figure 5.30). Even within a range of such small measurements, it could be said that glued timbers behaved somewhat more uniformly.

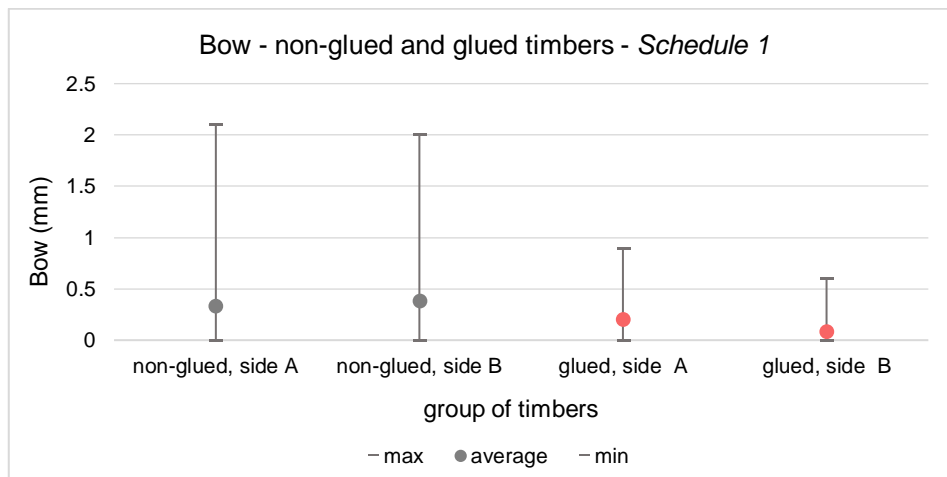
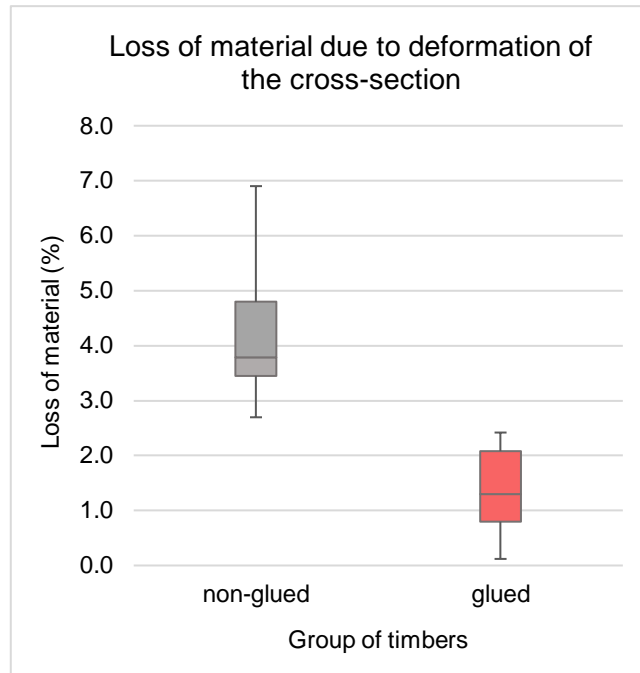


Figure 5.30. Bow - non-glued and glued timbers - Schedule 1.

## 5.4 Material loss due to cross-sectional deformation

As anticipated, a cross-sectional deformation of non-glued units was considerably higher compared to the glued ones. While all four sides were usually deformed on non-glued timbers, the deformation on glued timbers occurred mostly on two tangential sides. More consistent results of deformation were recorded within a group of glued timbers. The loss of material ranged from 2,7 % to 6,9 % and from 0,1 % to 2,4 % for non-glued and glued timbers respectively, so even the maximal loss among glued units was lower than the minimum loss among non-glued. The quartiles are illustrated in Figure 5.31.



**Figure 5.31. Material loss due to deformation of the cross-section; Quartiles.**

The material loss averaged 4,1 % for non-glued and 1,4 % for glued units. Consequently, a saving of 2,7 % of dried material was achieved.

Twist and bow were not included in the calculation. However, having in mind that these deformations are lesser on glued timbers, but also given the higher density of examined glued timbers, one can only presume even greater material savings had twist and bow been taken into account.

Figure 5.32 and Figure 5.33 depict rhombic deformation, common for non-glued timbers, and a rather uniform shrinkage of glued units. Inner rectangle represents the cross-section of the final product. The wood outside of it would be the loss of material.



**Figure 5.32. A scan of the cross-section for material loss assessment (non-glued).**

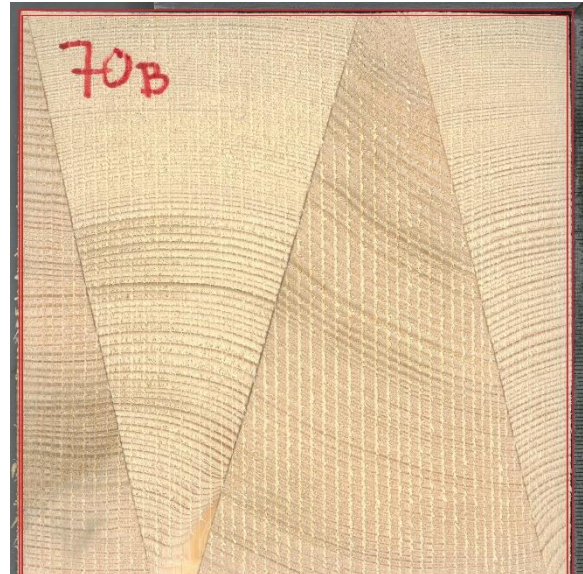


**Figure 5.33. A scan of the cross-section for material loss evaluation (glued).**

## 5.5 Case-hardening

Differing results of case-hardening after one and after five days of conditioning indicate that one day long conditioning was not enough to completely equalize moisture content of a specimen. Higher values of case-hardening were measured on glued specimens (*Figure 5.35*). However, since the initial MC and density varied considerably, it is difficult to infer whether it was gluing or alternating positions of sections within a single glued timber that made a significant contribution to the increase of residual stresses. The most probable reason is the position of cambial rings in glued timbers. The quartiles of measured values are plotted in *Figure 5.34* and *Figure 5.35*.

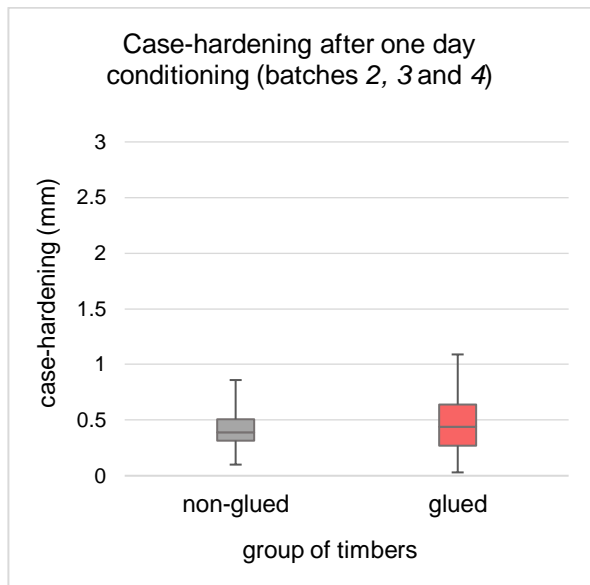


**Figure 5.34. Case-hardening after one day conditioning (batches 2, 3 and 4); Quartiles.**

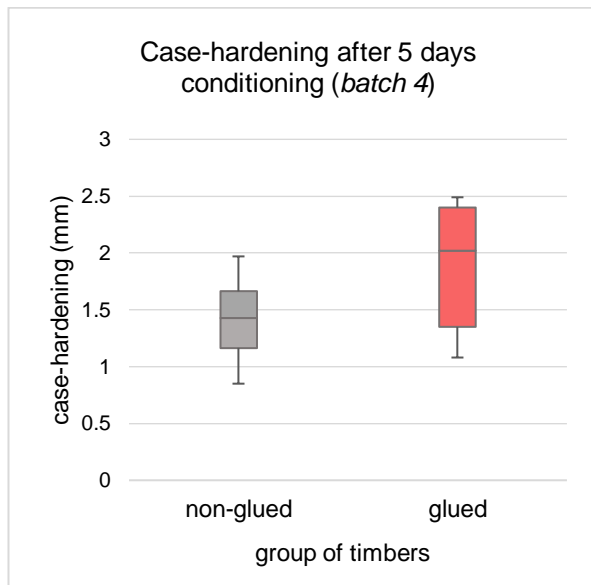


**Figure 5.35. Case-hardening after 5 days conditioning (batch 4); Quartiles.**

## 5.6 Checks

Recorded amount of checks and the sum of their lengths varied quite inconsistently from one schedule to another as well as between non-glued and glued timbers. Based on such incongruities, little could be deduced regarding whether one schedule was qualitatively better than others.

### 5.6.1 Surface checks

The mean total length of surface checks per timber for all four schedules was 15,5 % lower for non-glued than for glued timbers. It averaged 42,5 cm compared to 50,2 cm respectively. However, these values could be misleading, since data of non-glued timbers was considerably skewed. *Figure 5.36* indicates that the median was significantly lower than the average. One half of non-glued timbers demonstrated values under 15 cm. The discrepancy was caused by an especially high amount of surface checks on some timbers, which increased the mean value significantly. The median of glued drying units was much closer to the mean and amounted to 43,8 cm. The maximum value was somewhat lower for glued timbers. On the other hand, almost 25 % of non-glued timbers were nearly free of checks. It should be noted, though, that many non-glued units, despite having no or just a few surface checks, had quite severe diagonally-oriented inner checks, some of which spanned though the whole piece from one front end to another (*Figure 5.37*). Moreover, both density and initial moisture content were lower for non-glued drying units, which most likely influenced the results.

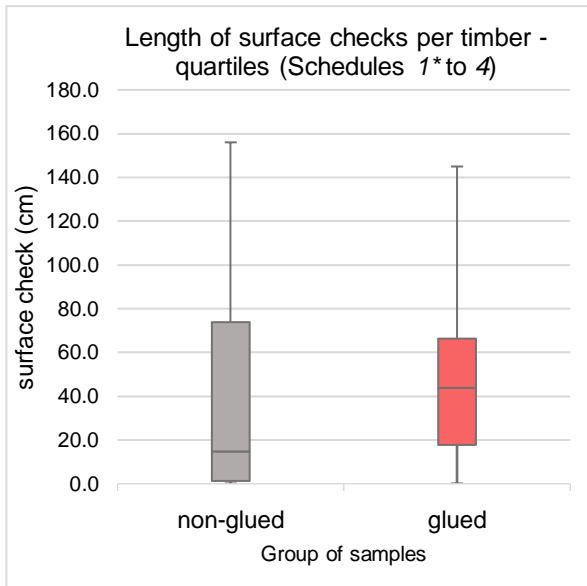


**Figure 5.36. Length of Surface Checks per Timber - Quartiles (Schedules 1\* to 4).**

\*The values for Schedule 1 are divided by 3.

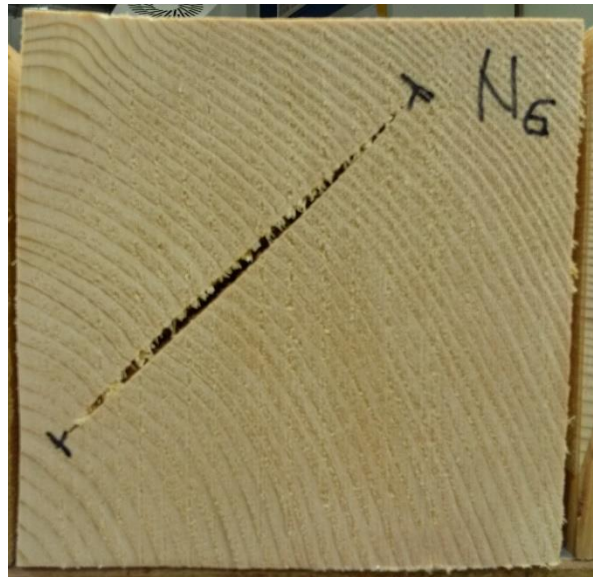


**Figure 5.37. A typical diagonally-oriented inner check in a non-glued timber.**

Figure 5.38 and Figure 5.39 represent lengths of surface checks per timber, summed and sorted by subtype for each drying schedule. Measured values of the first batch were divided by 3 (Schedule 1\*), in order to be comparable to the other three batches. Blue columns illustrate the summed lengths of all subtypes together, giving the average amount of surface cracks per timber and schedule. As displayed, mean values are quite inconsistent, indicating the effect of initial moisture content, wood structure and previous position in cross-section of the log. The mean values of glued units are comparable to those of non-glued ones, except for *Schedule 3*. Although, the basic density of non-glued timbers from the third batch was 20 % lower. The other three columns (orange, gray and yellow) in *Figure 5.38* and *Figure 5.39* indicate a clear distinction between non-glued and glued units. While most of the surface checks of glued timbers appeared due to nearly pure drying shrinkage, what had a dominant impact on the check formation of non-glued units were primarily the pith and secondly the knots. Besides, a high share of *checks reaching the front* for the last three schedules compared to *Schedule 1* indicate a significant effect of the length of drying units on check formation. A number of checks stretched from one end to another end of shorter drying timbers, suggesting that more rapid front drying probably fostered check propagation. This might be an explanation for comparable amounts of checks between *Schedule 1* and the remaining three schedules, despite higher moisture gradients throughout and at the end of *Schedule 1*.

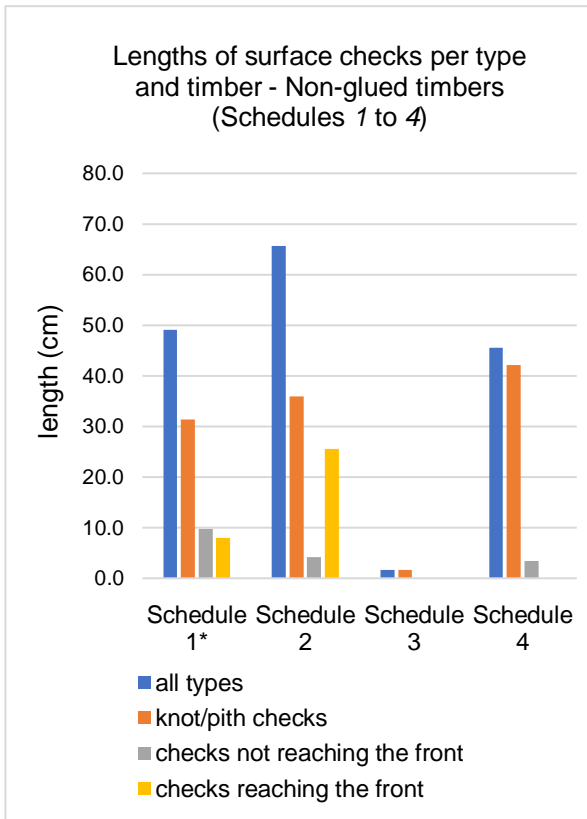


**Figure 5.38. Lengths of surface checks per type and timber - Non-glued timbers (Schedules 1 to 4).**  
\*The values for Schedule 1 are divided by 3.

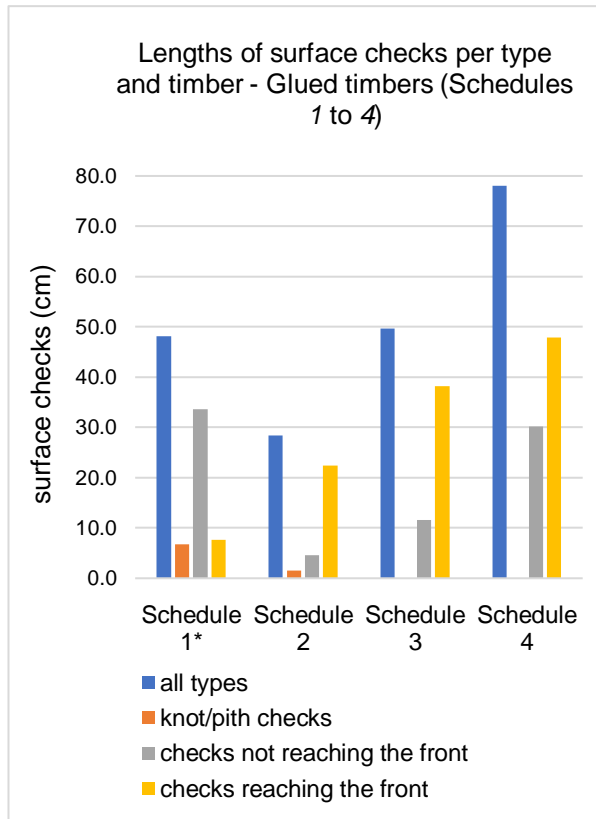


**Figure 5.39. Lengths of surface checks per type and timber - Glued timbers (Schedules 1 to 4).**  
\*The values for Schedule 1 are divided by 3.

## 5.6.2 End checks

Quite high values of end checks were recorded. The mean summed check length on both ends for all four batches amounted to 22,7 cm for non-glued and 33,1 cm for glued units. The quartiles are presented in Figure 5.40. Discrepancy between the median of non-glued and glued units was higher compared to the mean. Although the minimum to maximum range was similar, the interquartile range was lower for glued timbers, suggesting higher uniformity within the group.

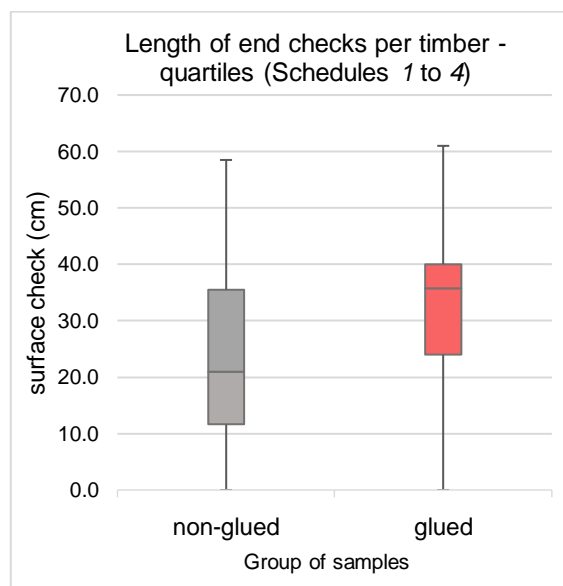


**Figure 5.40. Length of End Checks per Timber - Quartiles (Schedules 1 to 4).**

Figure 5.41 displays mean and median values for each schedule, both for non-glued and glued units. Generally, both mean and median values were lower in case of non-glued timbers, except for Schedule 2. However, consistency between mean and median values within a group was higher for glued timbers.

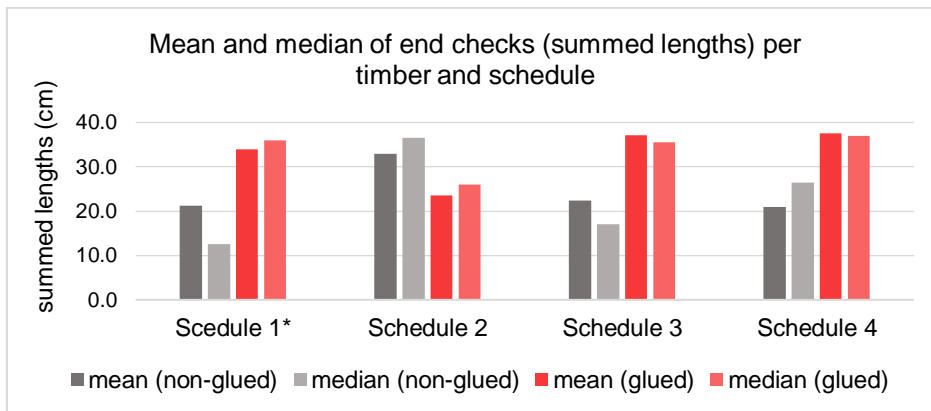


Figure 5.41. Mean and median of end checks (summed lengths) per timber and schedule.

### 5.6.3 Frequency of checks and length classification

Both surface and end checks were measured and classified according to their length. Figure 5.42 shows the mean number of surface checks per timber organized in four length classes. Gray columns represent non-glued, while orange columns depict glued drying units. There were no checks shorter in length than 2,0 cm. In the remaining three classes glued timbers exhibited slightly higher values. Check lengths between 5,0 and 20,0 cm were most frequent for both groups.

Figure 5.43 displays the average number of end checks per timber for all four schedules together, sorted in three categories as follows: 0-2, 2-5 and 5-15 cm. The number of checks was evenly distributed throughout the categories, except for the middle one in which checks for glued units doubled, being roughly four compared to two. Moreover, quite a high number of large checks for both non-glued and glued timbers was detected.

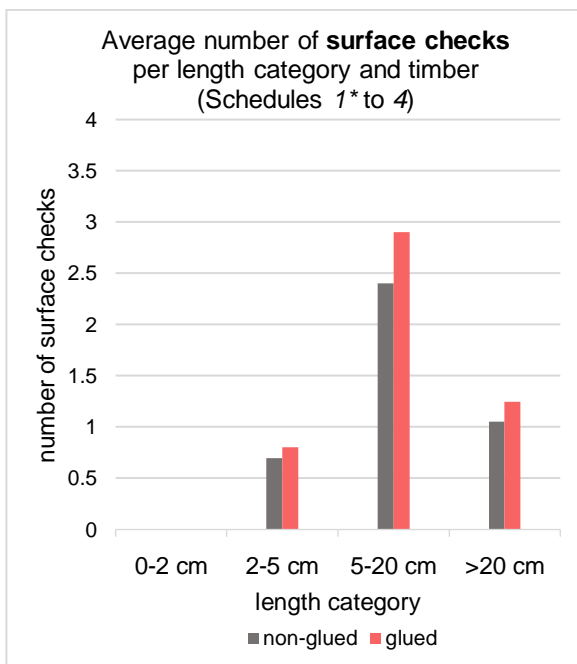


Figure 5.42. Average number of surface checks per length category and timber (Schedules 1\* to 4).  
\*The values for Schedule 1 are divided by 3.

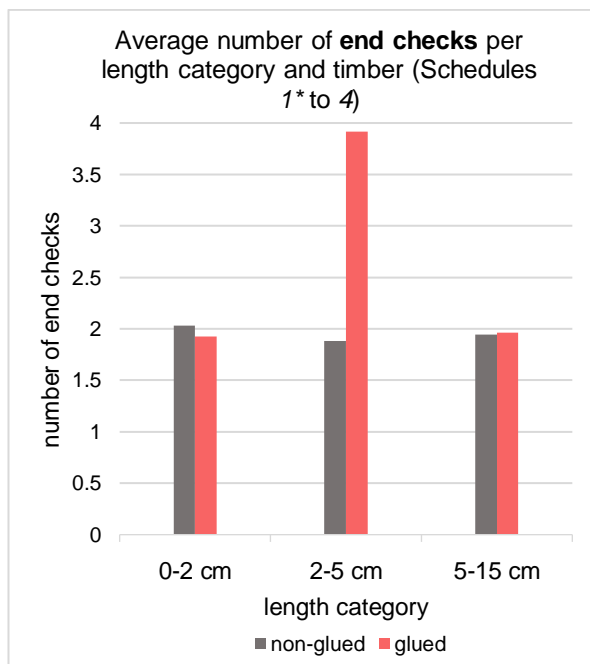


Figure 5.43. Average number of end-checks per length category and timber (Schedules 1\* to 4).  
\*The values for Schedule 1 are divided by 3.

**5.6.4 Distribution of checks and general description**

A distinctive characteristic of glued timbers was the distribution of surface checks. Due to the specific position of sections within a drying unit, always giving two almost pure tangential and two radial faces of the timber, nearly the entire amount of surface checks was located on two tangential sides; leaving the radial ones almost completely free of checks. The distribution is shown in *Figure 5.44*. On the other hand, check distribution for non-glued timbers varied considerably and depended mostly on the previous position in the cross-section of the log.

The shape of checks and the position of end checks in relation to outer edges of the drying unit were distinctive between non-glued and glued units as well. Since almost all checks were radial ones, position of annual rings within a timber was a critical factor. Therefore, the end checks of glued timbers were almost vertically positioned, mostly propagating from the tangential surface toward the center of the piece. Furthermore, the checks were always positioned in the inner two sections of timber (*Figure 5.45*). On the other hand, position and shape of checks in non-glued timbers varied a great deal. For pith-containing non-glued timbers the checks were quite unpredictable, usually vertically or horizontally positioned. They were very deep and wide, commonly accompanied by twist deformation. Non-glued timbers without pith predominantly had annual rings diagonally positioned within a unit. Hence, the checks were mostly diagonally positioned, perpendicular to cambial rings. Many of them, although severe, were inner checks, not visible on the side faces. This was due to the highest mass of wood tissue located in the center of timber, looking radially along the check, hence the check emerged in the central zone and propagated toward the outer zones.

Although not measured on every drying unit, much wider checks were noticed on non-glued timbers. While the width among glued units was rather uniform, varying around 1,0 mm and not exceeding 2,0 mm, it reached as much as 10,0 mm among non-glued units, significantly deforming the timber (*Figure 5.46*).

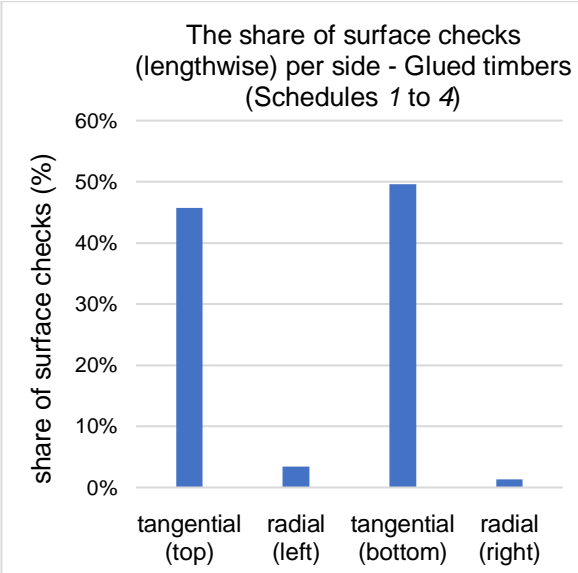


**Figure 5.44.** The share of surface checks (lengthwise) per side - Glued timbers (Schedules 1 to 4).



**Figure 5.45.** A typical position of checks in glued timbers.

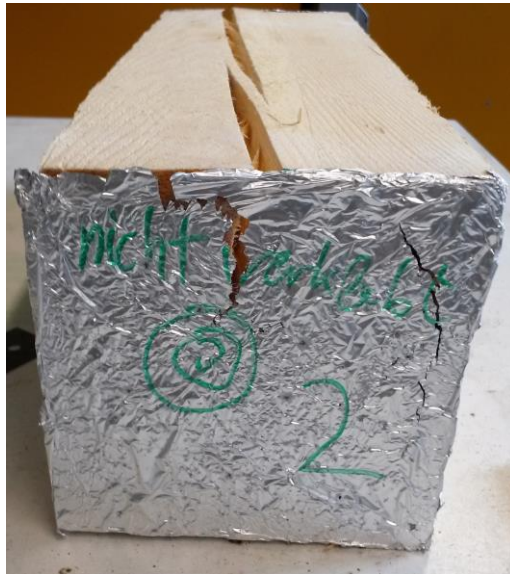


**Figure 5.46.** A typical wide check in a pith-containing non-glued timber.

## 6 Discussion

### 6.1 Schedule

As previously mentioned, drying schedules conducted in this study were quite harsh. Such a high level of severity was selected on purpose, having in mind the impact of drying time on the capacity of the mill. The aim was to determine whether it is possible to dry wet glued timbers in a comparable period of time to non-glued timbers. The drying times varied from 254 to 283 hours. The reduction in drying time from the first to the last schedule was recorded, despite lowering the drying parameter values. Factors such as variation in wood structure, initial moisture content, and distribution of water in a single timber could be a possible explanation for this inconsistency (Pang 2002; Sonderegger et al. 2011). Furthermore, an issue during the first drying program (*Chapters 5.1 and 6.2*) and a switch in kilns afterwards could be additional reasons for prolonged drying in the first run.

Schedules 1 to 4 were much more severe than those of Glos and Wagner (1988), Welling and Mieth (1989) and Rémond (2004), especially at the beginning of drying (*Table 1; Table 2; and Table 4*). For the moisture content range from “green” to 60 % the equilibrium moisture content (EMC) was set between 11,0 % and 13,7 % in the reviewed literature, whereas it was set to 9 % in the current study. Furthermore, at the moisture content of around 35 %, the EMC ranged from 10,0 to 13,7 in the reviewed literature (*Table 1; Table 2*). In comparison, EMC in this study was set to 7,1 % during the first two schedules and 8,1 % during the last two (*Table 4; Table 5*). Consequently, the drying time was much shorter in this study than in Glos and Wagner (1988). Considering the lesser thickness of the board in Rémond (2004), drying time would likely be much higher if one was to simulate drying of timbers 140 to 150 cm thick. Duration of drying in Welling and Mieth (1989) was around 230 hours. However, it is unclear which specimens were used for controlling the schedule, since lumber of quite diverse dimensions was dried simultaneously. Furthermore, there is no information on final moisture content of the specimens.

According to Rémond (2004), lowering the gap between dry-bulb and wet-bulb temperatures does not necessarily mean prolonged drying. It should extend the first phase of drying (*Chapter 2.4*), keeping the evaporating front close to the surface and allowing water from deeper zones to move more rapidly out of the wood. Consequently, moisture gradients and internal stresses would be milder. Therefore, there is perhaps a possibility of lessening moisture gradients and alleviating stresses by lowering the psychrometric gap in the first part of conducted drying schedules, without additionally sacrificing time.

### 6.2 Drying

The average measured final moisture contents (MC) of non-glued and glued timbers were comparable. On the one hand, non-glued timbers exhibited lower MC after the first two schedules, due to lower initial MC. The difference in wood density have to be considered as well, as glued timbers generally exhibit a slightly higher values due to the specific sawing pattern. On the other hand, glued timbers showed slightly lower moisture contents after *Schedule 3* and *Schedule 4*. Almost all units were over-dried, as a result of high moisture variation among drying units and inaccurate on-line moisture measurements (*chapters 5.2.1.2 and 6.4*). The same problem was recorded in Glos and Wagner (1988).

The results showed quite a similar drying manner of non-glued and glued timbers. Very much alike drying rates of both groups of timber were recorded for units with similar basic density, initial MC, and moisture distribution (*Figure 5.12; Figure 5.13*). However, these three parameters considerably influenced the drying rate. Timbers with higher initial MC and basic density dried slower. Non-glued *N3 – run 3G* (light orange dots; *Figure 5.5*) dried slower than glued *39B – run 3G* (dark orange dots), despite the same initial MC, but instead as a result of

lower basic density. Steiner (2008) recorded a nearly linear drop in drying rate with the increase in wood density of Norway spruce. On the other hand, faster drying of glued 70B – run 2G timber (dark blue dot, *Figure 5.5*) than non-glued N4 – run 2G (light blue dot) was observed, due to different moisture distribution within the piece, even though initial MC was higher. A larger amount of free water in the middle heartwood zone of non-glued timber significantly decelerated the drying process. Heartwood pits are generally aspirated (Keey & Nijdam 2002; Pang 2007), hence the permeability is considerably reduced. Furthermore, the amount of free water in heartwood is in the zone of irreducible saturation, a state where liquid flow continuity is broken (Nijdam et al. 2000) and saturated tracheids are “trapped” by surrounding empty tracheids. In such a case, capillary movement is hindered and diffusion becomes the predominant drying mechanism. All observed timbers, both non-glued and glued, confirmed such slow drying of free water from the heartwood zone (*Figure 5.6*). Slower drying in the deeper sapwood zone (*Chapter 5.2.3; Figure 5.11 - Segment 7*) could also be the consequence of pit aspiration, this time because of drying (*Chapter 2.5*), and irreducible saturation. Another possible reason for delayed drying in this zone is discussed later.

Moisture distribution measurements at the end of last three drying schedules showed no distinctive differences (*Figure 5.14*). This was probably due to mild parameter changes between schedules. However, much better clustering was achieved when it was done after the origin of the timber (*Figure 5.15*), pointing out the impact of initial MC and wood anatomy on both drying and shape of the moisture distribution curve. When averaged, moisture distribution curve was quite similar for both non-glued and glued timbers. Although the range between minimum and maximum curves was much higher for glued timbers. This is mostly due to variation in initial MC rather than lower drying rates. The total number of observed units, which was 4 for non-glued and 11 for glued timber, additionally contributed to scattering. There were not many non-glued timbers with such high, or comparably high, initial moisture content as that of glued timbers, which eventually influenced the end results considerably. Nevertheless, an open question remained – a question of probability of very high moisture content in a single non-glued piece of timber, or more specifically that of very high MC in deeper zones as well as a high net amount of water in a whole piece. Since the cutting pattern plays a significant role, it is somewhat possible that non-glued timbers generally have lower average moisture content than glued timbers. In that case, it could be said that drying of glued timbers is in general a more difficult process. Moreover, cutting patterns and log diameters used in a particular sawmill must be taken into account.

The higher moisture gradients recorded after *Schedule 1* are presumably influenced by the very low equilibrium MC, which was down to 4,3 % during the first 20 hours of drying. This caused, almost certainly, over-drying of the outer zone and receding of the evaporation front, simultaneously confining the capillary water in deeper zones. Consequently, the moisture gradients were increased and drying time prolonged.

### 6.3 The effect of glue lines

No moisture accumulation near the glue lines was recorded (*Chapter 5.2.4*). *Specimen 2* (*Figure 5.22*) did not display any distinguishing disturbances in drying. However, after analyzing segments *I, II, III, and IV* in *Specimen 3* (*Figure 5.23*), some hindering of drying was observed.

Sapwood dries faster than heartwood, but usually takes longer to dry to target MC due to higher initial MC (Pang 2007). However, sapwood segments *I* and *IV* from this study exhibited slightly lower MC after drying than heartwood segment *II* and *III* (*Chapter 5.2.4, Figure 5.24; Figure 5.25*). Therefore, one could assume that a certain obstacle due to narrowing of glue lines is present. Nevertheless, MC of wood at the narrowest part of the corresponding section, near the pith, is always low. Furthermore, moisture from the central part succeeds to diffuse at a comparable rate as in non-glued units (*Figure 5.12; Figure 5.13*), as mentioned previously. Therefore, it could be concluded that a slight diffusion barrier does not have a significant impact on drying.

However, the effect of glued layers and the alternating pattern of sections in glued timber on capillary flow should be considered for further inspection and analysis, since it could play an important role in cases where sapwood with high moisture content would reach deeper zones of a timber (Segments 3 and 7 in *Specimen 1*; *Figure 5.11*). Actually, since no liquid flow through the glue line is possible, and even if it were, the heartwood behind it would still be an obstacle because of the already interrupted capillary flow. Thus, a more precise question would be whether there is a significant amount of capillary water in segments 3 and 7 that would flow tangentially if there was no glue line and/or crossed heartwood part. It could be presumed, though, that the impact is not major, since capillary movement from even deeper segments 4, 5 and 6 was recorded (*Figure 5.11*).

## 6.4 Resistance vs gravimetric method

A rather substantial discrepancy between gravimetric and resistance moisture measurements was observed. High inaccuracy of resistance meters was noticed with moisture contents above FSP. These results corroborate the findings of Welling and Mieth (1989). According to Hartley and Marchant (1995), resistance meters give a good approximation of MC between 6 % and 25 %. The limitation, however, is not in their inability to measure resistance between electrode contacts out of the given range, but instead in the low accuracy of the calibration relationship between resistance and moisture content (Hartley & Marchant 1995).

Other than moisture content, moisture distribution within a single timber considerably influenced the variation between two methods. The resistance meters give a local estimation of MC. Therefore, if the MC at the measuring point varies from the MC in other parts of the piece, the results will differ from the mean MC. When drying thick lumber these differences are quite significant, making a traditional way of drying-schedule controlling, by estimating mean MC, quite unreliable. In this study timbers with relatively low initial moisture content and free water in the zone close to the wood surface showed the highest inaccuracy at the beginning of the schedule (*Figure 5.5*). On the contrary timbers with higher initial moisture content showed the highest variance after five days of drying. At this point in time periphery of the timber dried considerably. This caused a significant drop in average moisture content measured by the gravimetric method. On the other hand, there was still a high amount of water in deeper parts of timber, which caused higher MC values measured by the resistance meter, since it always measures the highest MC along the length of the electrode contact. Extreme results were recorded for timbers with high initial MC in deeper sapwood zones, displaying MC values of 50 to 60 % even after nine days of drying (*Figure 5.8*), despite the actual average MC being around 30 % and about 15 % in segments 1 and 9. Glos and Wagner (1988) experienced similar problems. Such measurements left almost no possibility for estimation of internal stresses during drying. Furthermore, they led to over-drying of almost every single timber in all four batches.

The usage of mean MC to control drying schedules gives satisfying results when drying thin boards, since moisture gradients are relatively mild. However, when drying thick timbers a different approach to the problem is required. One possible way to overcome this issue would be to apply electrode contacts of different lengths, as well as insulated contacts specifically for deeper parts of the timber. Although the resistance method is not particularly appropriate for measuring moisture distribution due to its low accuracy above FSP (Teischinger & Vanek 1987), the on-line determination of moisture distribution in thick lumber, by using contacts of various lengths and insulated contacts, should give much better insight than average MC measuring into how different parts of the piece dry, hence providing better evaluation of internal stresses. Moreover, more subtle controlling of the schedule would be possible. Given that different electrodes are particularly important in different drying phases, their selection for schedule-controlling (i.e. electrodes with short screws in sapwood during first days of drying and those with longer contacts later on) would open up the possibility to focus on different drying mechanisms, thus lessening the internal stresses without prolonging drying time significantly.

Additional divergence between the two measuring methods was possible due to different measuring locations on a single follow-up timber in case of the gravimetric method (*Chapter 4.2.2.2*).

## 6.5 Checks and internal stresses

Quite a high amount of checks on both non-glued and glued timbers was observed. Nevertheless, the total length of checks per piece was much lower than in Welling & Mieth (1989). However, the number of check-free surfaces was lesser than in Glos & Wagner (1988), implying that drying conditions in this particular study were more severe. Check-free surface count was as follows: 2,4 and 2,5 per timber for non-glued and glued units respectively, compared to 2,4 for cross-section 14 x 24 cm and 3,3 for cross-section 8 x 18 cm in Glos & Wagner (1988). Unfortunately, further quantitative comparison could not be drawn due to different measuring methods. In general, non-glued timbers were less prone to checking than glued ones. This applies to both surface and end checks. This, but also increased case hardening, was probably due to nearly pure tangential sides in glued timbers. However, non-glued timbers generally had wider checks, reaching up to 10 mm on timbers containing pith, as opposed to maximal 2 mm on glued units. Position of checks was highly dependent on the previous position in the cross-section of the log, making glued timbers much more consistent and predictable. Moreover, the negative effect of pith and knots was evidently reduced due to the alternating pattern of adjacent sections of glued timbers, exhibiting almost solely clear checks as a result of tangential shrinkage. Both of the aspects mentioned above allowed better focus on drying schedule optimization.

As noted earlier, position of annual rings within a timber was of crucial importance and a key factor for the shape and location of checks in timber. Centrally positioned, pith containing, timbers exhibited severe vertically and/or horizontally positioned checks, propagating from the surface toward the center of the timber (*Figure 5.46*). On the other hand, timbers with diagonally positioned annual rings were prone to inner checks, stretching diagonally, perpendicular to annual rings (*Figure 5.37*). This was most likely due to the highest mass of wood tissue located in the center of timber, looking radially along the check, hence the check emerged in the central zone and propagated toward the outer zones. Pith and knots affected check formation considerably, demonstrating distinctive weak points of the non-glued timbers (*Figure 5.38*).

In case of glued timbers, checks were mostly vertically positioned in two inner sections, propagating from the tangential side toward the central zone of the timber. This implied that drying conditions were severe during the first few days. Most likely due to high psychrometric gap, and hence too intensive evaporation, capillary forces were not able to supply the evaporating front with free water from the inner zones. Consequently, there was a receding of the front toward the central zones of the timber, hindering the gradient independent, capillary flow. As a result, very high gradients were formed, followed by stresses exceeding the tension strength of the wood in the outer zones. In addition, receding of the evaporative front slowed down the drying process considerably. "Trapped" liquid water from deeper zones was forced to move out of the drying unit by much slower diffusion. Additionally, irreducible saturation (*Chapter 2.4*) (Salin 2008; Nijdam et al. 2000; Wiberg et al. 2000; Wiberg & Moren 1999), as well as reduced permeability due to pit aspiration (*Chapter 2.5*) (Comstock & Côté 1968; Liese & Bauch 1967) certainly had a great impact on the cease of liquid flow and withdrawal of the evaporative front. Lowering the psychrometric gap during the first days of drying could prolong the first, constant, much faster, and perhaps most importantly gradient-independent drying phase dominated by capillary forces (Rémond 2004). This should significantly relieve the tension in the outer zone and consequently reduce the amount of checks.

Glos & Wagner (1988) and Mauritz & Vanek (1992) reported a great impact of "relieving" grooves on check-formation in thick lumber dried at conventional temperatures. Introduction of similar or even shallower centrally positioned grooves on the wider side of each section of glued timbers would probably reduce check-formation. The deformation of grooves would be

most likely lower than in Glos & Wagner (1988), due to almost pure tangential deformation parallel to the correspondent surface.

The results of Mauritz & Vanek (1992) showed radical reduction of checks in timbers of comparable dimensions by conducting high-temperature drying. High temperature could also have a positive effect on glued timbers, due to an increase in convective moisture migration. However, reported discoloration, smell, and wood degradation should be considered.

Preliminary results of radio frequency/vacuum drying of glued beams, with almost twice as large cross-sectional area, conducted at the *Institute of Wood Technology and Renewable Materials (BOKU)* showed almost complete prevention of surface checks, indicating a major effect of convective vapor migration and targeted heating on reduced stress development in outer zones of wood. However, inner checks were still present to a considerable extent.

## 7 Conclusion

The results in this study proved that drying of wet-glued timbers with quite harsh drying schedules at conventional temperatures is possible. The target moisture content was reached at a rate comparable to non-glued timbers. However, initial moisture content, wood density and moisture distribution had a critical effect on the drying rate. Moisture gradients were similar for non-glued and glued timbers of alike density, moisture distribution and initial MC. A minor impact of glue lines on moisture diffusion was recorded (*Chapter 5.2.4; Figure 5.25*). However, this effect proved to be of almost no significance to the drying rate of a whole timber, due to favorable moisture distribution within a single section of a glued drying unit (*Chapter 6.3*).

Although mean twist values of non-glued and glued timbers were very low and comparable, a huge improvement was observed when maximum values were set side by side. A specific cutting pattern and alternating position of sections within a single glued unit significantly weakened the negative impact of pith on twist deformation, without sacrificing much of the material. Bow deformation was negligible for both non-glued and glued timbers. Lower mean and maximum values for glued timbers indicate, though, positive effects of gluing and alternating position of the sections.

Loss of material due to cross-sectional deformation was much less in case of glued timbers. It reached maximum of 2,4 % compared to 6,9 % for non-glued units. On average a saving of 2,7 % dried material was achieved, not including twist and bow deformation. If these factors, as well as lower density of non-glued timbers were considered, the saving would be even higher.

Greater case hardening was observed on glued timbers. Amount of surface and end checks was higher for glued units as well, very likely due to nearly pure tangential shrinkage in one of the two orthogonal directions of the cross section. However, the increase in checks was not major. The sum of surface checks per timber was similar after *Schedule 1* and even lower after *Schedule 2*. This is a great encouragement for further optimizing, having in mind great improvements regarding yield and deformation, as well as uniformity of the product.

### 7.1 Further research

Future research regarding the influence of reduced psychrometric gap in the first phase of drying is highly recommended; the focal point should be the effect it has on reduction of check-formation and duration of drying (*Chapter 6.5*). Furthermore, a research could also be done regarding interference with and discontinuity of the liquid flow path when drying thick lumber. On the one side, there is the impact of irreducible saturation and pit aspiration. On the other side, there is the extent of severity of the drying schedule, a factor that can be controlled. More details on these aspects would shed light on ways in which the capillary flow can be prolonged. Despite it certainly being a challenging task, this kind of research would provide insight into how much room for manoeuvre there is for potentially improving and optimizing drying schedules.

Moreover, further comparisons of non-glued and glued timbers with high initial moisture content are needed, since the number of non-glued timbers with high MC in this study was very limited. More precisely, the question at hand is whether there is a significant amount of capillary water in segments 3 and 7 (*Figure 5.11; Figure 5.3*) that would flow tangentially if there was no glue line and/or crossed heartwood part. Möttönen and Kärki (2010) and Möttönen, Kärki, and Martikka (2011) used a dye solution to trace liquid migration in wood. Besides, a question of probability of very high moisture content in a single non-glued unit, or more specifically that of very high MC in deeper zones should be addressed as well. It is possible that glued timbers generally have more free water in deeper zones (Segments 3 and 7, *Figure 5.3*).

Preliminary results obtained at the *Institute of Wood Technology and Renewable Materials, BOKU* regarding lessening the tension in the outer zone of a drying unit, and hence the reduction of surface checks in glued beams by applying radiofrequency/vacuum drying, are more than satisfying and justify further optimizing of the drying schedule in order to reduce the extent of honeycombing. Furthermore, very promising results of Mauritz and Vanek (1992) after conducting high-temperature drying on non-glued timbers of similar cross-section (*Chapter 6.5*) indicate that similar tests on glued units could provide a solution for the reduction of checks in glued units.

The effect of “relieving” grooves, discussed in *Chapter 3*, on check-formation in glued timbers and beams would be interesting to test as well.

## 8 References

- Brackwell, P. & Walker, J.C.F., 2006. Sawmilling. In *Primary wood processing: principles and practice*. Dordrecht: Springer, pp. 203–250.
- Choong E T, 1965. Diffusion coefficients of softwoods by steady-state and theoretical methods. *Forest Products Journal*, 15(1), pp.21–27.
- Comstock, G.L. & Côté, W.A., 1968. Factors affecting permeability and pit aspiration in coniferous sapwood. *Wood Science and Technology*, 2(4), pp.279–291.
- Fronius, K., 1982. Arbeiten und Anlagen im Sägewerk, Band 1. - Der Rundholzplatz, Stuttgart: DRW-Verlag.
- Fronius, K., 1989. Arbeiten und Anlagen im Sägewerk, Band 2. - Spaner, Kreissägen, Bandsägen, Stuttgart: DRW-Verlag.
- Fronius, K., 1991. Arbeiten und Anlagen im Sägewerk, Band 3 - Gatter, Nebenmaschinen, Schnitt- und Restholzbehandlung, Stuttgart: DRW-Verlag.
- Glos, P. & Wagner, L., 1988. Untersuchung zur technischen Trocknung von Fichtenschnittholz mit großen Querschnittsabmessungen, Stuttgart: Fraunhofer IRB Verlag.
- Hansmann, C. et al., 2002. Permeability of wood - A review. *Drevarsky Vyskum/Wood Research*, 47(4), pp.1–16.
- Hartley, J. & Marchant, J., 1995. Methods of determining the moisture content of wood, Beecroft: Research Division - State Forests of New South Wales.
- Hawley, L.F., 1931. Wood-liquid relations, Technical bulletin no. 248, Washington, D.C.: U.S. Dept. of Agriculture.
- Kang, H.Y. & Hart, C.A., 1997. Temperature effect on diffusion coefficient in drying wood. *Wood and Fiber Science*, 29(4), pp.325–332.
- Keey, R.B. & Nijdam, J.J., 2002. Moisture movement on drying softwood boards and kiln design. *Drying Technology*, 20(10), pp.1955–1974.
- Kolin, B., 2000. Hidrotermička obrada drveta 2nd ed. B. Šoškić & G. Danon, eds., Belgrade: Jugoslavijapublik, Belgrade.
- Liese, W. & Bauch, J., 1967. On the closure of bordered pits in conifers. *Wood Science and Technology*, 1(1), pp.1–13.
- Mauritz, R. & Vanek, M., 1992. First results with high temperature drying of large sized structural wood. *3rd IUFRO Drying Conference, 1992 Vienna*, pp.374–378.
- Möttönen, V. & Kärki, T., 2010. Tracing the migration of liquid water and wood extractives in silver birch and Scots pine sawn timber during drying using a dye solution. *Wood Material Science and Engineering*, 5(2), pp.116–122.
- Möttönen, V., Kärki, T. & Martikka, O., 2011. Method for determining liquid water flow in wood during drying using a fluorescent dye tracer. *European Journal of Wood and Wood Products*, 69(2), pp.287–293.
- Mouchot, N. et al., 2006. Characterization of diffusional transfers of bound water and water vapor in beech and spruce. *Maderas. Ciencia y tecnología*, 8(3), pp.139–147.
- Nijdam, J.J., Langrish, T.A.G. & Keey, R.B., 2000. A high-temperature drying model for softwood timber. *Chemical Engineering Science*, 55(18), pp.3585–3598.
- ÖNORM EN 13183-1: Feuchtegehalt eines Stückes Schnittholz - Teil 1: Bestimmung durch Darrverfahren, February 2004.
- ÖNORM EN 13183-2: Feuchtegehalt eines Stückes Schnittholz - Teil 2: Schätzung durch elektrisches Widerstands-Messverfahren, July 2002.
- ÖNORM ENV 14464: Schnittholz - Verfahren zur Ermittlung der Verschalung, July 2002.

- Pang, S., 2002. Effects of sawing pattern on lumber drying: model simulation and experimental investigation. *Drying Technology*, 20(9), pp.1769–1787.
- Pang, S., 2007. Mathematical modeling of kiln drying of softwood timber: model development, validation, and practical application. *Drying Technology*, 25(3), pp.421–431.
- Pang, S., 1998. Relative importance of vapour diffusion and convective flow in modelling of softwood drying. *Drying Technology*, 16(1–2), pp.271–281.
- Rémond, R., 2004. Approche déterministe du séchage des avivés de résineux de fortes épaisseurs pour proposer des conduites industrielles adaptées. Doctoral thesis. Engineering Sciences [physics]. ENGREF (AgroParisTech).
- Rémond, R., Perré, P. & Mougel, E., 2005. Using the concept of thin dry layer to explain the evolution of thickness, temperature, and moisture content during convective drying of norway spruce boards. *Drying Technology*, 23(March), pp.249–271.
- Rosner, S. et al., 2010. Radial shrinkage and ultrasound acoustic emissions of fresh versus pre-dried Norway spruce sapwood. *Trees - Structure and Function*, 24(5), pp.931–940.
- Ross, R.J. ed., 2010. Wood handbook: Wood as an engineering material, Madison, WI: U.S. Dept. of Agriculture, Forest Service, Forest Products Laboratory.
- Salin, J., 2010. Problems and solutions in wood drying modelling: history and future. *Wood Material Science & Engineering*, 5(2), pp.123–134.
- Salin, J.G., 2008. Drying of liquid water in wood as influenced by the capillary fiber network. *Drying Technology*, 26(5), pp.560–567.
- Schulte, P.J., Hacke, U.G. & Schoonmaker, A.L., 2015. Pit membrane structure is highly variable and accounts for a major resistance to water flow through tracheid pits in stems and roots of two boreal conifer species. *New Phytologist*, 208(1), pp.102–113.
- Siau, J.F., 1984. Transport processes in wood. Springer series in wood science, Berlin Heidelberg New York Tokyo: Springer-Verlag.
- Simpson, W.T. ed., 1991. Dry Kiln Operator's Manual, Madison, WI: U.S. Dept. of Agriculture, Forest Service, Forest Products Laboratory.
- Skaar, C., 1988. Wood-water relations. Springer series in wood science, Berlin Heidelberg New York London Paris Tokyo: Springer.
- Sonderogger, W. et al., 2011. Combined bound water and water vapour diffusion of Norway spruce and European beech in and between the principal anatomical directions. *Holzforschung*, 65(6), pp.819–828.
- Steiner, Y., 2008. Optimizing the air velocity in an industrial wood drying process, Master thesis. Department of Ecology and Natural Resource Management. Norwegian University of Life Sciences.
- Teischinger, A., 2012. Trocknung. In A. Wagenführ & F. Scholz, eds. *Taschenbuch der Holztechnik*. Carl Hanser Verlag, pp. 433–456.
- Teischinger, A. & Vanek, M., 1987. Eignung verschiedener Auftrennmethode zur Bestimmung eines Feuchtegradienten im Holz nach Darmmethode. *Holzforschung und Holzverwertung*, 39, pp.5–8.
- Usta, I. & Hale, M.D., 2006. Comparison of the bordered pits of two species of spruce (Pinaceae) in a green and kiln-dried condition and their effects on fluid flow in the stem wood in relation to wood preservation. *Forestry*, 79(4), pp.467–475.
- Vanek, M. & Teischinger, A., 1989. Diffusionskoeffizienten und Diffusionswiderstandszahlen von verschiedenen Holzarten. *Holzforschung und Holzverwertung*, 41(1), pp.3–6.
- Walker, J.C.F., 2006. Primary wood processing: Principles and practice 2nd ed., Dordrecht: Springer.
- Welling, J. & Mieth, S., 1989. Einfluß der Nadelstichperforation auf die Rißbildung in

Fichtenholz, Stuttgart: Fraunhofer IRB Verlag.

Wiberg, P. & Moren, T.J., 1999. Moisture flux determination in wood during drying above fibre saturation point using CT-scanning and digital image processing. *Holz als Roh- und Werkstoff*, 57(2), pp.137–144.

Wiberg, P., Sehlstedt-P, S.M.B. & Morén, T.J., 2000. Heat and mass transfer during sapwood drying above the fibre saturation point. *Drying Technology*, 18(8), pp.1647–1664.